Chem. Soc. Rev., 1986, **15**, 405—448

Fluorescence Decay Dynamics of the Halogens and Interhalogens

By Michael C. Heaven *
DEPARTMENT OF CHEMISTRY, ILLINOIS INSTITUTE OF TECHNOLOGY, CHICAGO, IL. 60616, USA

1 Introduction

The diatomic halogens and interhalogens show a wide variety of photochemical [1,2] and chemiluminescent [2,3] behaviour. This interesting facet of their chemistry has provided the motivation for decades of careful spectroscopic study of this family of molecules. The initial investigations were mostly concerned with the static properties of the electronic states, *i.e.* the assignments and the precise energies of the rotational, vibrational, and electronic (ro-vibronic) states. Much progress has been made in this field, and the principal visible and infra-red electronic transitions for all of the halogens and interhalogens, with the exception of F_2, are known.[1] Although there are considerable differences in the amount and quality of the spectroscopic data available for each molecule, they are, taken as a family, better characterized than any other group of closely related diatomics.

The photochemical and chemiluminescent properties of the halogens and interhalogens are largely determined by the dynamic properties of the ro-vibronic states (*i.e.*, rates for radiative transitions, spontaneous dissociation, collisional excitation and deactivation, *etc.*). The electronic transitions for these molecules fall in an experimentally convenient spectral region, providing ideal prototypes for the investigation of the elementary steps of photochemical and chemiluminescent reactions. In recent years additional motivation for such studies has come from the recognition that some of the chemiluminescent reactions may be used to produce a chemically-driven electronic transition laser.[4]

The dynamic properties of the ro-vibronic states can be determined from the fluorescence decay characteristics. However, in order to obtain meaningful data it is essential to be able to examine the properties of individual rotational and vibrational states. For many years it was a technically difficult matter to observe the state-resolved dynamics, so this information was usually estimated from absorption line-strength measurements and kinetic modelling of chemiluminescence spectra. Direct probing of the excited-state dynamics became technically feasible with the advent of high power, tunable laser sources. Several investigators

* Address after September 1, 1986: Department of Chemistry, Emory University, Atlanta, GA 30322, USA

[1] J. A. Coxon, in 'Molecular Spectroscopy', ed. R. F. Barrow, D. A. Long, and D. J. Millen, Specialist Periodical Reports, The Chemical Society, London, 1973, Vol. 1, p. 177.
[2] See, for example, H. Okabe, 'Photochemistry of Small Molecules', Wiley-Interscience, New York 1978.
[3] R. D. Kenner and E. A. Ogryzlo, in 'Chemi- and Bioluminescence', ed. J. G. Burr, Marcel Dekker, 1985, p. 45.
[4] M. A. A. Clyne and I. S. McDermid, in 'Dynamics of the Excited State', ed. K. P. Lawley, John Wiley, 1982, p. 1.

have used laser excitation to study the dynamic behaviour of the halogens and interhalogens, and a large data base of fluorescence decay lifetimes, quenching rate constants, and ro-vibrational energy-transfer rate constants has been assembled.[5]

The present review will not attempt to give a summary of this extensive field. Instead, the intention is to provide a description of the work carried out in this area by the late Michael A. A. Clyne and his collaborators. This group conducted systematic studies of the fluorescence decay dynamics of chlorine, bromine, and all of the interhalogens with the exception of ClF. Their results and conclusions provide an excellent self-contained description of the various excited-state decay mechanisms, while the range of molecules studied was sufficient to illustrate the major trends within the halogen/interhalogen family. Some of the experimental methods (and pitfalls) will also be presented.

Clyne's group studied the halogens and interhalogens by laser excitation techniques over a period of five years. Throughout this time the experiments and the methods of data analysis were continually improved. Insights gained in the study of each new molecule were applied to re-evaluate the data for previously studied molecules, and the measurements of the lifetimes, quenching rate constants, and energy-transfer rate constants were systematically refined. This review will try to preserve some of the logical progression of this evolution. However, before embarking on a detailed account of these experiments a summary of the spectroscopic and dynamic theory relevant to the low-lying electronic states of the halogens and interhalogens will be presented.

2 The Visible and Near Infra-red Electronic Transitions of the Halogens and Interhalogens

A. Halogens.—The electronic states which arise from the combination of two ground-state halogen atoms ($Z\,np^5 + Z\,np^5$, where $n = 2, 3, 4$, and 5 for Z = F, Cl, Br, and I respectively) have been described by Mulliken.[6–8] A simple linear combination of atomic orbitals (LCAO) model predicts that σ_g, π_u, π_g^* and σ_u^* molecular orbitals (MO's) will be formed from the atomic p orbitals, as shown in Figure 1. The family of valence electronic states correspond to the permutation of the 10 valence electrons among these molecular orbitals. Mulliken[6] has labelled each configuration by the digits which represent the occupation numbers for the four orbitals. Thus the lowest energy configuration $(\sigma_g)^2(\pi_u)^4(\pi_g^*)^4(\sigma_u^*)^0$ (*cf.* Figure 1) is designated as 2440, and this is the $X\ ^1\Sigma_g^+$ ground state. Promotion of one of the π_g^* electrons gives the first excited configuration, 2431, from which the electronic states $^1\pi_u$ and $^3\pi_u$ are derived. Many other electronically excited states are readily predicted using this simple MO model, and those belonging to some of the lower energy configurations are shown schematically in Figure 2. This diagram also shows the qualitative energy ordering of the configurations, the spin–orbit splitting of the molecular states, and the resolution

[5] J. I. Steinfeld, *J. Chem. Phys. Ref. Data*, 1984, **13**, 445.
[6] R. S. Mulliken, *Phys. Rev.*, 1934, **46**, 549.
[7] R. S. Mulliken, *Phys. Rev.*, 1940, **57**, 500.
[8] R. S. Mulliken, *J. Chem. Phys.*, 1971, **55**, 288.

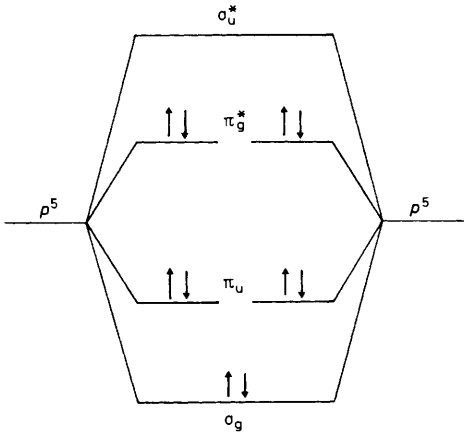

Figure 1 *Molecular orbitals for the valence shell configurations of the diatomic halogens. The configuration illustrated is the* 2440 $^1\Sigma_g^+$ *ground state*

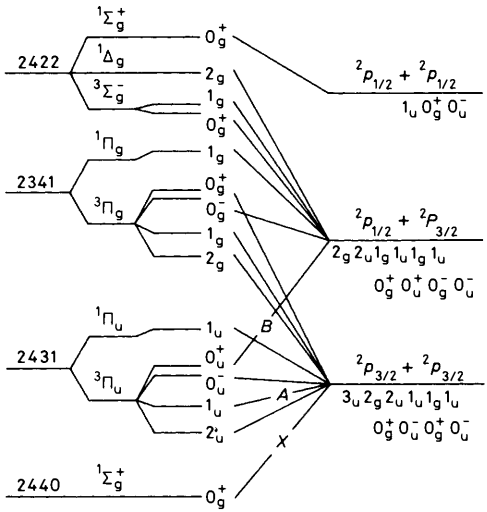

Figure 2 *Correlation diagram for the low-lying halogen valence shell states with their predicted dissociation products. The correlations are based on symmetry conservation and the non-crossing rule for states of the same angular momentum*

of each state into its multiplet components[9] (these are labelled by the Ω quantum number, which represents the projection of the total electronic angular momentum along the internuclear axis). The left-hand side of Figure 2 corresponds to Hund's case (a) coupling of the electronic angular momenta. This assumes that the atomic

[9] G. Herzberg, 'Molecular Spectra and Molecular Structure. Part 1, Spectra of Diatomic Molecules', Van Nostrand, New York, 1950.

spin and orbital angular momenta (S and L) are uncoupled from one another, and coupled separately to the internuclear axis. However, for the halogens (and interhalogens) this approximation is only valid at very small internuclear distances. At the distances which are typical of the equilibrium bond lengths (r_e), the atomic spin–orbit coupling is still partially effective. As a consequence, the molecular spin and orbital angular momenta (Σ and Λ) are not well defined, and Ω ($= |\Lambda + \Sigma|$) is the only meaningful quantum number. This situation is known as Hund's case (c), and it gives the best description of the coupling at intermediate and large internuclear distances.[6]

Spin–orbit coupling in the atoms splits the np^5 configuration into a $^2P_{\frac{3}{2}}$ ground state and a $^2P_{\frac{1}{2}}$ excited state. The separation between these states increases with increasing nuclear charge, and the splittings range from 404 cm^{-1} for F to 7 603 cm^{-1} for I. Mulliken[6–8] has shown how the atomic states combine to give the various molecular Ω states. Three combinations are possible for the halogens; $Z\ ^2P_{\frac{3}{2}} + Z\ ^2P_{\frac{3}{2}}$, $Z\ ^2P_{\frac{1}{2}} + Z\ ^2P_{\frac{3}{2}}$, and $Z\ ^2P_{\frac{1}{2}} + Z\ ^2P_{\frac{1}{2}}$ The molecular states belonging to each combination are indicated on the right hand side of Figure 2. Correlation between the case (a) multiplets and the case (c) states can be made on the basis that Ω is a valid quantum number at all internuclear distances, and that states with the same symmetry and Ω value cannot cross.

It is known from both experimental and theoretical work that the majority of the states show in Figure 2 are repulsive (anti-bonding).* Apart from the ground state, the most deeply bound states correlate with the 2431 $^3\Pi_u$ configuration. These are usually given the labels $B\ ^3\Pi(0_u^+)$, $A^3\Pi(1_u)$, and $A'\ ^3\Pi(2_u)$ [the Ω values are not subscripted, to emphasize the mixed case (a)/case (c) nature of the states]. Transitions between the ground state and the A and B states are responsible for the visible and near infra-red spectra of the halogens.[1] Although the transitions are formally spin-forbidden, they are observed. Much of their intensity can be ascribed to the extensive mixings of the molecular singlet and triplet states, which are mediated by the persistence of the atomic spin–orbit coupling.[7] For example, the A—X transition is enhanced by the mixing of $A\ ^3\Pi(1_u)$ with the nearby $^1\Pi(1_u)$ state. Similarly the B—X transitions gain intensity from the mixing of $B\ ^3\Pi(0_u^+)$ with 1441 $^1\Sigma(0_u^+)$; and the mixing of $X\ ^1\Sigma(0_g^+)$ with 1342 $^3\Pi(0_g^+)$. The interactions between the 0^+ states are very effective in promoting the B—X transitions and these are always much stronger than the A—X systems.

The $^3\Pi_u$ states are less strongly bound than the ground state, and a typical halogen absorption spectrum consists of long vibrational progressions of the B—X and A—X systems. At shorter wavelengths these progressions merge into continuum absorptions. A third continuum absorption, belonging to the 2431 $^1\Pi(1_u)$—X transition, also appears in the short wavelength region. To illustrate this situation, a potential energy diagram for Br_2 is shown in Figure 3, where the range of Franck–Condon accessible transitions from the vibrationless level of the ground state have been indicated.

* Above the states shown in Figure 2 lie many bound ion-pair and Rydberg states, but these are not considered here.

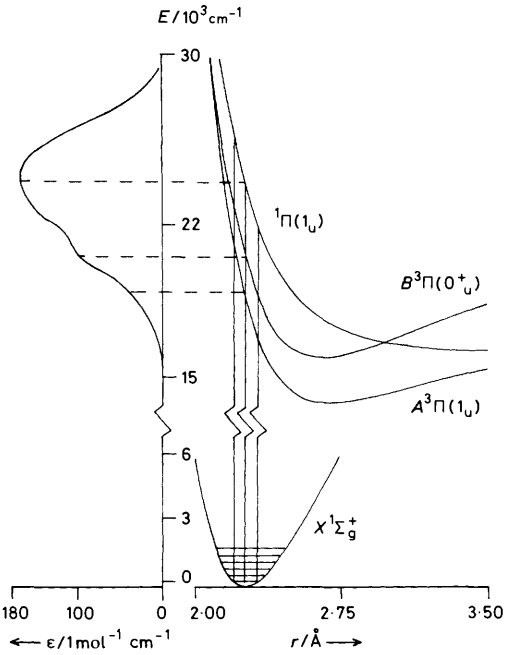

Figure 3 *Potential energy curves and continuum absorption spectrum for* Br_2. *Transitions from the vibrationless level of the X state are also shown as a set of vertical lines. The central line shows the most probable transitions, while the lines on either side show the range of transitions which occur from* $v'' = 0$. *The broken horizontal lines show how the maxima in the continuum spectrum correspond to the highest probability transitions from* $v'' = 0$.

B. Interhalogens.—The low energy electronic states of the interhalogens are analogous to those of the halogens, but there are two important differences; the u—g symmetry element does not exist, and there are two different dissociation limits which correlate with a spin–orbit excited atom ($Y\ ^2P_{\frac{1}{2}} + Z\ ^2P_{\frac{3}{2}}$ or $Y\ ^2P_{\frac{3}{2}} + Z\ ^2P_{\frac{1}{2}}$). These differences do not affect the X, A', and A states significantly, but they do change the character of the B state. Despite the loss of the u—g symmetry, the B states of the interhalogens still formally correlate with one of the $Y\ ^2P_{\frac{1}{2}} + Z\ ^2P_{\frac{3}{2}}$ dissociation limits. They are, however, more or less strongly perturbed by a repulsive 0^+ state [usually labelled as $Y(0^+)$] which correlates with ground-state atomic products[10] (this perturbation is symmetry-forbidden in the halogens). In the heavier interhalogens (*e.g.* IBr, ICl) the interaction is strong enough to cause an avoided crossing. This forces the B state to correlate with ground-state products, and a new bound-state is formed above the crossing point [usually designated $B'(0^+)$]. Figure 4 shows the relevant potential energy curves for IBr. The broken lines represent the diabatic potential energy curves in the limit of an allowed crossing. The full lines represent the adiabatic potential curves which

[10] M. S. Child and R. B. Bernstein, *J. Chem. Phys.*, 1973, **59**, 5916.

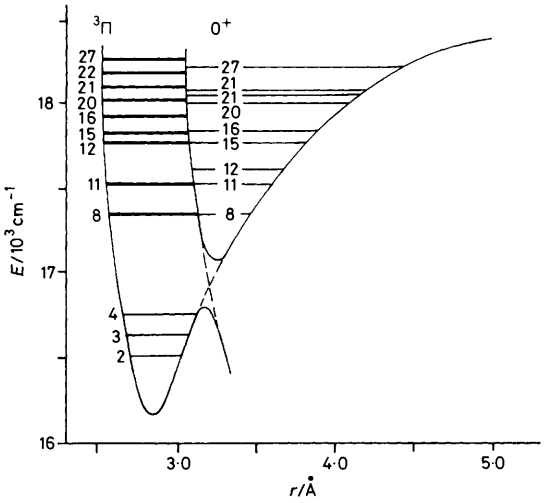

Figure 4 *Potential energy curves for the $B\,^3(0^+)$ and $B'(0^+)$ states of* IBr. *The heavy horizontal lines indicate the positions of vibrational levels to which transitions have been observed* (Reproduced by permission from *Ark. Fys.*, 1962, **21**, 529)

are the result of an avoided crossing. IBr shows the best example of this behaviour, with other interhalogens exhibiting properties which are more consistent with partially avoided crossings. For a useful semi-quantitative description of these curve crossings for the whole family of interhalogens, see Child and Bernstein.[10]

As for the halogens, the principal low energy electronic transitions of the interhalogens are the A—X and B—X systems. Again, the B—X system is the more intense, to the extent that the A—X system is only known reliably for IBr, ICl, and IF.[4] The vibrational energy level spacings of the *B* states always show anomalies caused by the $Y(0^+)$ state perturbations. Analysis of these data has provided information concerning the interaction strengths and the positions of the crossing points. At energies appreciably above the crossings, the *B* states are strongly predissociated (*i.e.* dissociation occurs at energies below the diabatic dissociation limit), and, with the exception of ClF(*B*), the vibrational quantization is largely destroyed. The near u.v. spectra of the interhalogens are dominated by continuous absorptions to a number of different states, though most of these have not yet been characterized in any detail.

3 Radiative Decay, Predissociation, and Collisional Relaxation

Fluorescence decay measurements provide information concerning a wide variety of radiative and non-radiative processes.[11] The spontaneous (non-collisional) decay channels available to an excited diatomic molecule can be described using the potential energy curves shown in Figure 5. Consider the case where a single vibrational level, which lies at an energy below the ground state dissociation limit,

[11] J. N. Demas, 'Excited State Lifetime Measurements', Academic Press, New York, 1983.

has been excited. Provided that internal conversion to the ground state is negligibly slow, the decay rate for this level will be determined solely by the rate at which the molecules radiate to the ground state. This rate is equivalent to the Einstein coefficient for spontaneous emission ($A_{v'}$), and it determines the radiative lifetime ($\tau_r = 1/A_{v'}$). The A_v coefficient is the sum of the rates for all of the radiative transitions (these are shown as a vibrational progression from $v' = 0$ in Figure 5). It is defined by the relationship:[2]

$$A_{v'} = \frac{64\,\pi^4}{3h} \sum_{v''} |R_e|^2\, q_{v',v''}\, \nu^3_{v',v''} \qquad (1)$$

where R_e is the electronic transition dipole moment and $q_{v',v''}$ is the Franck–Condon factor for the v'—v'' band* which occurs at frequency $\nu_{v',v''}$. $|R_e|^2$ is a more fundamental measurement of the transition probability than the radiative decay rate, and values for this parameter are usually calculated from experimentally determined lifetimes. Unfortunately, there is some difficulty in using equation 1 for this purpose. The Franck–Condon factors must be known for all of the transitions which contribute to the radiative decay. In most instances these are not accurately

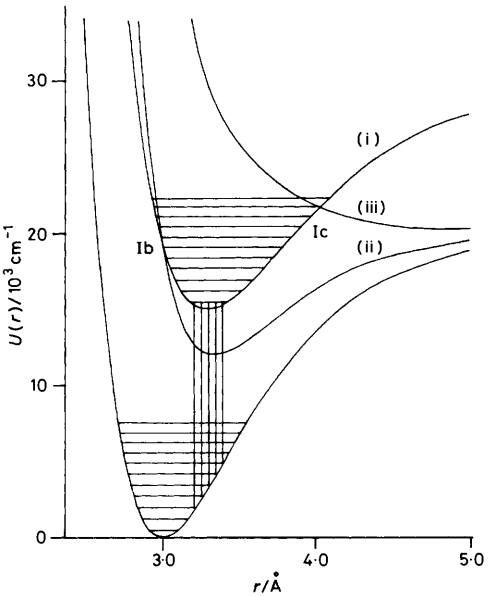

Figure 5 *Potential energy diagram showing a radiative vibrational progression from* $v' = 0$ *of state* (i) *to the ground state, a type* Ib *crossing between states* (i) *and* (ii), *and a type* Ic *crossing between states* (i) *and* (iii). *See text for details*

* For electronic transitions, it is customary to list the higher energy state first and labelled with one prime (*i.e.* v', J'), and the lower energy state second and labelled with a double prime (*i.e.* v'', J''). Changes in the appropriate quantum number follow the same convention: *i.e.* $\Delta v = v' - v''$; $\Delta J = J' - J''$.

known for transitions to very high vibrational levels of the ground state, but reasonable estimates can be made based on the extrapolation of experimentally determined potential energy curves. A more serious problem is posed by the dependence of $|R_e|^2$ on the internuclear separation. The mean distance at which a particular $v' - v''$ transition occurs (the *r*-centroid, often denoted by $\bar{r}$) is a function of v' and v''. Consequently, $|R_e|^2$ in equation 1 is dependent on v'', and the exact form of the dependence is unknown for the majority of the halogens and interhalogens. However, the range of *r*-centroids spanned by the most intense components of a vibrational progression is normally quite small, and it is often assumed that $|R_e|^2$ is approximately constant for emission from a single vibrational level, so that

$$A_{v'} = \frac{64\,\pi^4 |R_e|^2\,(\bar{\nu})^3}{3h} \tag{2}$$

where $(\bar{\nu})^3$ is defined by $(\bar{\nu})^3 = \sum_{v''} q_{v',v''}\,\nu^3_{v',v''}$. Values for $|R_e|^2$ may thus be obtained from the experimentally derived lifetimes using equation 2.

Excited-state vibrational levels lying above the ground-state dissociation limit may be subject to predissociation.[9,12,13] Two diabatic curve crossings are shown in Figure 5, either of which could cause predissociation if the selection rules for non-radiative transition are satisfied. For Hund's case (c) these are as follows:

$$\Delta\Omega = 0, \pm 1;\ u \longleftrightarrow u;\ g \longleftrightarrow g;$$

$$\Delta J = 0;\ + \longleftrightarrow +;\ - \longleftrightarrow -$$

In addition, the strength of the interaction will be proportional to the Franck–Condon overlap between the bound and repulsive states.[14] Predissociations with $\Delta\Omega = \pm 1$ are termed heterogeneous, and they are forbidden in the absence of molecular rotation ($J' = 0$). Mixing between such states is mediated by the coupling of electronic and rotational motion, and the strength of interaction is directly proportional to the rotational energy.[13] Predissociations with $\Delta\Omega = 0$ are termed homogeneous and are allowed for rotationless states.[10]

Predissociation provides a non-radiative decay channel which shortens the observed fluorescence decay lifetime (τ_0) such that

$$\frac{1}{\tau_0} = \frac{1}{\tau_r} + \Gamma_p$$

where Γ_p is the predissociation rate. The quantum yield for fluorescence ($\Phi_F = \tau_0/\tau_r$) is also diminished by predissociation, and in the limit that $\Gamma_p >> 1/\tau_r$ emission from the excited state becomes undetectably weak. This fact has often been used to detect the presence of predissociation, and in favourable instances the

[12] R. S. Mulliken, *J. Chem. Phys.*, 1960, **33**, 247.
[13] M. S. Child, in 'Molecular Spectroscopy', ed. R. F. Barrow, D. A. Long, D. J. Millen, Specialist Periodical Reports, The Chemical Society, London, 1974, Vol. 2, p. 466.
[14] J. Tellinghuisen, in 'Photodissociation and Photoionization', ed. K. P. Lawley, John Wiley, 1985, p. 299.

observed energy threshold for the onset of predissociation can be used to determine a close upper limit for the lower state dissociation energy.[9] For example, Figure 5 shows a curve crossing between an excited state (i) and the repulsive limb of a second bound state (ii), at an energy below the dissociation limit of the latter. In this situation the first level of state (i) lying above the dissociation limit for state (ii) will be predissociated [Herzberg's[9] case I(b)]. Predissociations caused by curve crossings which occur at energies significantly above the lower state dissociation limit are not so informative [*cf.* the crossing between states (i) and (iii) in Figure 5]. Here the onset of predissociation indicates only an upper limit for the dissociation energy [Herzberg's[9] case I(c)]. Experimentally, the details of a curve crossing [case I(b) or I(c)] can be deduced from the subtle effects of rotational motion on the onset of predissociation.[9,12]

Collisional quenching of an electronically excited state can also contribute to the observed fluorescence decay rate. Empirically, quenching can be described in terms of an overall rate constant (k_m) for deactivation of excited molecules, so that

$$\frac{1}{\tau_0} = \frac{1}{\tau_r} + \Gamma_p + k_m[M] \qquad (3)$$

where [M] is the concentration of the quenching species. This allows for the determination of the quenching rate constant from the slope of a plot of $1/\tau_0$ *vs.* [M] (Stern–Volmer plot).[15] Equation 3 is frequently used to determine collision-free lifetimes from data taken under significantly quenched conditions. Unfortunately, Stern–Volmer plots often show deviations from linearity, especially at low concentrations, and the lifetimes obtained by linear extrapolation can contain very large errors. This problem arises because collisional deactivation can proceed by a number of competing pathways. For example, the halogen and interhalogen *B* states are deactivated by both direct and indirect mechanisms. Direct deactivation involves a collision-induced transition to a non-emitting electronic state, while the indirect process occurs by collisional promotions of the molecules to predissociated levels within the *B* state, followed by dissociation. Apart from these intrinsic difficulties, measurements of fluorescence decay lifetimes, under both collision-free and collisional conditions, can be subject to serious instrumental distortion. These problems will be discussed after a description of the experimental techniques has been given.

4 Experimental Techniques

The majority of the lifetime data for the halogen and interhalogen *B* states were obtained by direct observation of the fluorescence decay. In a typical experiment, fluorescence was initiated by using a short duration light pulse to excite the *B*—*X* system. Selective excitation of individual ro-vibrational levels (v',J') was essential because the predissociated *B* states have lifetimes which are strongly varying functions of v' and J' (indeed, in the early studies of the I_2 and Br_2 *B* state lifetimes, the excitation of overlapped spectral features produced a number of apparently

[15] O. Stern and M. Volmer, *Z. Phys.*, 1919, **20**, 83.

conflicting results). The quantum state dependence of the lifetime also imposes severe limits on the pressures which can be used for lifetime determinations. Rotational and vibrational energy transfers are very efficient processes for halogen–halogen (or interhalogen–interhalogen) collisions, and the transfer between levels of differing lifetime causes deviation from linear Stern–Volmer behaviour, as described above. Consequently, the lifetimes must be measured at pressures which are low enough to permit collision-free observations. In practice the B state radiative lifetimes span a range from about 1 to 300 μs. Assuming gas-kinetic transfer rates, this means that the measurements should be made at pressures between 0.2 to 100 mtorr.

Selective and sensitive methods are required to excite and detect fluorescence from an individual ro-vibrational state under low pressure conditions. This is most effectively accomplished by use of the laser-induced fluorescence technique (LIF). Figure 6 shows an LIF apparatus which was used for many of the studies described here. Metered flows of the species of interest were admitted into a high vacuum chamber *via* a pin hole or leak valve. The molecules were excited by light pulses from a turnable dye laser, which typically operated with a linewidth of 0.03 cm^{-1}, a pulse duration of 10 ns, and a repetition frequency of 20 Hz. Fluorescence was detected along an axis which was perpendicular to the laser axis by a high gain photomultiplier tube. Inevitably a small fraction of the laser light was directly scattered into the detector. This was removed by a coloured glass filter which blocked the laser wavelength but transmitted the longer wavelength fluorescence. Signals from the photomultiplier were processed by either a boxcar integrator or a transient digitizer. The boxcar is, in essence, a sample-and-hold amplifier which can remove the random noise from a repetitive signal. On receiving a trigger pulse from the laser, the boxcar samples the signal from the photomultiplier for a preset interval (usually set to be the same as the fluorescence decay lifetime). The samples are integrated over several laser pulses, and the boxcar outputs a d.c. voltage which is directly proportional to the input voltage during the sampling interval. Although boxcars can be used to obtain time-dependent information, such as fluorescence decay curves, they are best suited for monitoring total fluorescence intensity. Transient digitizers are the fastest and most accurate instruments for recording fluorescence decays. These are basically high speed analogue-to-digital converters integrally connected to a digital memory. To capture a transient event the instrument is initially set continuously to digitize the input signal at a fixed sampling rate. Each time the signal is digitized the result is stored in the first memory location, and the memory addresses of the preceeding data points are incremented. The last (oldest) datum point is discarded. On receiving a trigger pulse the recorder digitizes a preset number of times and then stops. If this number is smaller than the memory size, the memory will contain some of the data taken before the trigger occurred. This facility to record pre-trigger information is very valuable because it allows for unbiased determination of the base line signal before the laser pulse. This level must be known accurately for a meaningful analysis of the decay characteristics. The data from a single laser pulse usually contain too much random noise to be used to determine a reliable lifetime. The noise is removed by

transferring the data to a computer where the results from a large number of laser pulses may be signal averaged. Once stored in the computer memory, the curves can be readily analysed by the appropriate fitting programs.

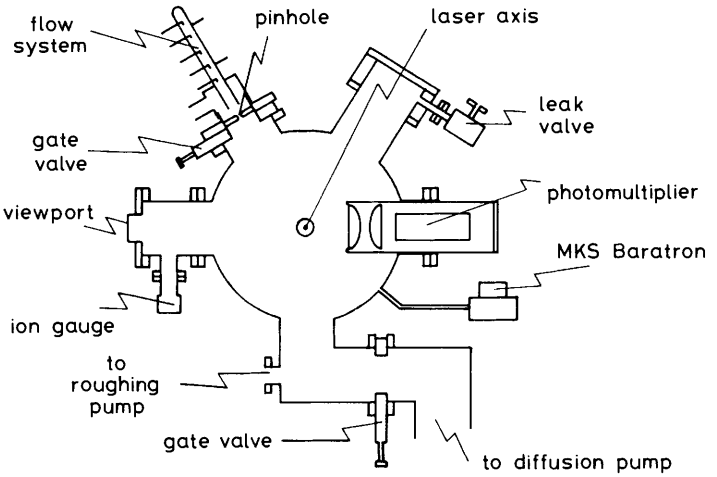

Figure 6 *Low-pressure fluorescence chamber showing the discharge-flow system for production of unstable species, and the fluorescence detection system*
(Reproduced by permission from *J. Chem. Soc., Faraday Trans. 2*, 1978, **74**, 1376)

In order to study lifetimes as a function of the vibrational and rotational quantum states it is necessary to identify unoverlapped spectral features and determine their quantum number assignments. Laser excitation spectra are recorded and used for this purpose. The spectrum is obtained by monitoring the fluorescence intensity as the laser is tuned through successive absorption features. This produces a trace which is similar to the absorption spectrum, but with the difference that transitions to predissociated levels are either anomalously weak or absent. A representative excitation spectrum for the IBr B—X system is shown in Figure 7. If the absorption spectrum has already been analysed, it is a straightforward matter to assign the lines of the excitation spectrum by direct comparison. The rotational and vibrational numbering given in Figure 7 was determined by this procedure. Previously unobserved band systems can be assigned by the method of combination differences.[9]

Another important facet of the excitation spectrum is that it provides the identity of the emitting species. Interhalogens exist in equilibrium with their constituent halogens or disproportionation products, and the species of interest is not always the most intensely emitting component of the mixture. Contamination by trace amounts of I_2, a strongly fluorescent molecule, has led to erroneous lifetime reports for IBr(B), ICl(B), and even $Br_2(B)$! Such complications are immediately obvious when adequately resolved excitation spectra are recorded.

The interhalogens IF and BrF present special experimental difficulties as they are

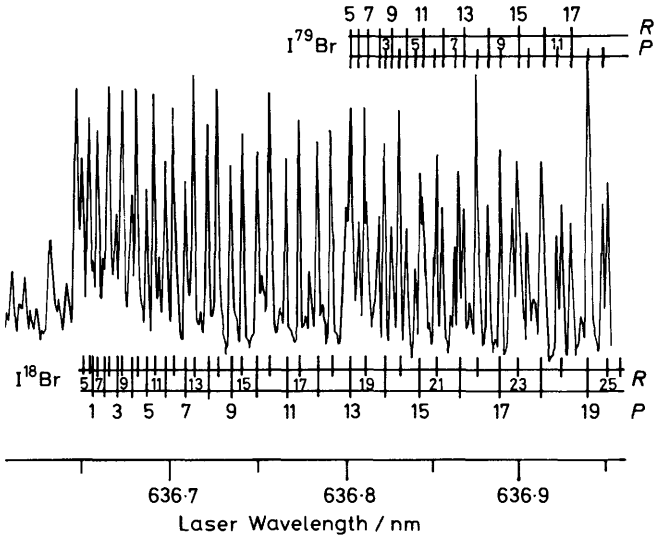

Figure 7 *Laser excitation spectrum of the* IBr (*B*—*X*) 3—3 *band, in the region of the* $I^{79}Br$ *and* $I^{81}Br$ *bandheads*
(Reproduced by permission from *J. Chem. Soc., Faraday Trans. 2*, 1980, **76**, 49)

both thermodynamically and kinetically unstable with respect to disproportionation. Useful steady-state concentrations of these molecules have been generated in a discharge flow system by the rapid reactions[16]

$$F + ICl \longrightarrow IF + Cl$$
$$F + Br_2 \longrightarrow BrF + Br$$

The F atoms were produced by the dissociation of F_2 in a microwave discharge. Unfortunately, the discharge flow system could not be operated at pressures which were low enough to permit collision-free measurements. This problem was solved by interfacing the flow system to a high vacuum fluorescence observation chamber. The essential components of this apparatus are illustrated in Figure 6. The flow system was maintained at pressures between 0.1—0.2 torr, allowing for stable operation of the microwave discharge and efficient production of the interhalogens. The reaction products were expanded through a pinhole into the chamber at a rate which produced total pressures of 0.5—1 mtorr.

5 Instrumental Distortion of Fluorescence Decay Curves

Some of the halogens and interhalogens have radiative lifetimes which exceed 50 μs, and at the low pressures (<2 mtorr) needed for collision-free measurement, diffusion can present a serious experimental difficulty. The excited molecules may

[16] M. A. A. Clyne and A. H. Curran, in 'Gas Kinetics and Energy Transfer', ed. P. E. Ashmore and R. J. Donovan, Specialist Periodical Reports, The Chemical Society, London, 1977, Vol. 2, p. 239.

either travel outside of the region observed by the detector, or they may be deactivated on the walls before emitting. This leads to an artificial shortening of the lifetime.[17,18] In the apparatus shown in Figure 6, diffusion of the molecules in a direction parallel to the laser axis does not influence the measurements. The cylinder of initially excited molecules extends well beyond the volume seen by the detector, and the net axial diffusion in and out of the viewing region is balanced. Radial diffusion can distort the fluorescence signals because molecules moving towards the photomultiplier are more efficiently detected than those moving away. Although the diffusion is symmetric, systematic errors are introduced as the detection efficiency is approximately proportional to the square of the distance from the photomultiplier. These errors can be minimized by positioning the detector at a large distance from the laser axis. However, the fraction of fluorescence collected falls dramatically as the distance is increased, and in practice a compromise distance which gives workable signals with minimal distortion must be found. Molecules can, of course, diffuse beyond the detection volume, but in the apparatus shown in Figure 6, deactivation of the excited molecules on the detector window was a more serious problem. For the unbiased recording of decay curves with lifetimes greater than 40 μs it was necessary to move the detector back from the laser axis.

Vibrational relaxation within the excited state is the cause of a more subtle instrumental distortion. In all instances the $^3\Pi$ states (*B*, *A*, and *A'*) have equilibrium internuclear separations which are greater than those of the ground states. The transitions with the largest Franck–Condon probabilities connect the high vibrational levels of the excited state with the low vibrational levels of the ground state and *vice versa* (*cf.* Figure 3). Laser excitation is therefore best suited for selective population of the high vibrational levels of the upper state, and these are prone to collisional vibrational relaxation. As the population relaxes down the vibrational ladder the fluorescence spectrum shifts to longer wavelengths in response to the change in the Franck–Condon distribution. This can cause a slight intrinsic change in the lifetime due to the modification of the $(\bar{\nu})^3$ term in equation 2. Of greater importance is the effect the spectral shift has on the detection efficiency. The sensitivity of the photomultiplier/coloured filter combination to fluorescence from a given vibrational level can be represented by the expression

$$S_{v'} = \sum_{v''} \Phi_\lambda \, q_{v',v''} \, \nu^3_{v',v''} \qquad (4)$$

where Φ_λ describes the variation with wavelength of the detection efficiency. Photomultiplier sensitivities fall rapidly as the long wavelength limit of the photocathode is approached, and the red-shifted fluorescence from vibrationally relaxed *B* (and *A*) state levels usually extends beyond this limit. Thus vibrational relaxation produces a time-dependent decrease of the detection efficiency, and the net result is a deviation from single exponential decay behaviour. The initial decay

[17] P. B. Sackett and Y. T. Yardley, *J. Chem. Phys.*, 1972, **57**, 152.
[18] P. B. Sackett, *Appl. Opt.*, 1972, **11**, 2181.

rate represents the combined effect of radiative decay, collisional deactivation, and vibrational relaxation. If the relaxation is fast compared with the other two processes, the vibrational population will eventually relax to an equilibrium distribution, and at long times the decay rate will slow down to the rate defined by the radiative and quenching channels. However, it is often the case that equilibrium is not achieved within a period of several fluorescence decay lifetimes, and the limiting decay rate cannot be observed. Under these conditions the decay curves must be analysed by computer modelling the convoluted response of the detector system to the time evolving fluorescence spectrum.

6 Laser-induced Fluorescence of the Halogens and Interhalogens

The absorption strengths of the *B*—*X* transitions are directly related to the radiative lifetimes of the *B* states; short lifetimes correspond to strong absorptions. Thus the short-lived *B* states ($\tau_r \leqslant 15$ μs) are the most easily excited and detected. In addition, the short lifetimes allow for relatively high pressures to be used for fluorescence decay measurement, while still maintaining effectively collision-free conditions. Iodine has the most intense *B*—*X* system and it has been studied by many research groups. Because the dynamics are so favourable and well characterized, the *B*—*X* system has been exploited for the development of new laser-based spectroscopic methods.[19,20] The literature concerning $I_2(B)$ is extensive, and the reader is referred to the works of Clyne and McDermid,[4] and Steinfeld[5] for further information.

The radiative decay rates ($\Gamma_r = 1/\tau_r$) of the halogens and interhalogens reflect the degree to which the spin quantization has been broken down by spin–orbit coupling. The coupling is greatest for the heaviest molecules, so these exhibit the

Table 1 *Radiative lifetimes[a] for the* $B\ ^3\Pi(0^+)$ *states of the halogens and interhalogens*

F_2	ClF	BrF	IF
b	350	56	7.0
	Cl_2	BrCl	ICl
	305	40	4.1
		Br_2	IBr
		12	1.4
			I_2
			1

Arrows indicate direction of increasing mass and spin–orbit coupling. [a] Lifetimes given in μs. The values quoted are for the lowest vibrational level studied for each molecule (typically $v' = 3$). [b] Bound levels of the F_2 *B* state have never been observed

[19] R. W. Field, *Faraday Discuss. Chem. Soc.*, 1981, **71**, 111.
[20] C. Kittrell, E. Abramson, J. L. Kinsey, S. A. McDonald, D. E. Reisner, R. W. Field, and D. Katayama, *J. Chem. Phys.*, 1981, **75**, 2056.

Table 2 *Collision–free fluorescence decay rates for the* $B^3\pi(0^+)$ *states of the halogens and interhalogens*[a]

	v'	$\Gamma_{00}/10^5 s^{-1}$	$k_{v'}/10^3 s^{-1}$	J'	*Ref.*
$I^{81}Br$					
	2	23	11	7—34	21
	3	140	21	3–32	21
$I^{35}Cl$					
	1	2.4	*s*	7—55	27
	2	2.4	1.0—4.3	7—54	27
	3	> 5000	*b*		29
IF					
	0	1.44	*s*	5—45	32
	1	1.49	*s*	3—49	32
	2	1.42	*s*	3—48	32
	3	1.45	*s*	3—50	32
	4	1.34	*s*	3—59	32
	5	1.23	*s*	3—57	32
	6	1.21	*s*	3—57	32
	7	1.16	*s*	4—57	32
	8	1.16	*s*	5—50	32
	9	1.14	*c*	0—6	32
	10	11	5.64	0—21	32
$^{79}Br^{81}Br$					
	2	0.806	*s*	4—31	38
	3	0.8	0.03	8—59	35
	4	0.8	5.0	6—26	35
	5	0.7[d]	25	1—20	35
	7	0.7[d]	*e*		
	11	0.6[d]	8.0	3—24	34,35
	14	0.6[d]	6.3	5—33	34,35
	19	0.5[d]	4.5	7—19	34,35
	20	0.5[d]	4.0	2—23	34,35
	23	0.4[d]	3.7	6—29	34,35
	24	0.4[d]	2.6	9—23	34,35
$^{81}Br^{35}Cl$					
	1	0.241	*s*	25	48
	3	0.24	*s*	15—35	46
	4	0.25	*s*	4—45	46
	5	0.25	*s*	6—60	46
	6	0.25	*s*	10—41	46
^{79}BrF					
	3	0.180	*s*	21	57
	4	0.169	*s*	21	57
	5	0.170	*s*	21	57
	6	0.160	*s*	10—45	57
	7	0.156	*s*	11—20	57
	8	5.71	40.2	4—21	56

Table 2—*cont.*

	v'	$\Gamma_{00}/10^5 s^{-1}$	$k_{v'}/10^3 s^{-1}$	J'	*Ref.*
$^{35}Cl_2$					
	5	0.033	*s*	16	61
	13	0.03[f]	770	0—5	63
	14	0.03[f]	590	0—5	62,63
	15	0.03[f]	530	0—7	62,63
	16	0.03[f]	410	0—7	62,63
	18	0.03[f]	380	0—7	62,63
	19	0.03[f]	420	0—7	62,63
	21	0.03[f]	290	0—7	62,63
	22	0.03[f]	240	0—7	62,63
	23	0.03[f]	160	0—7	62,63
	24	0.03[f]	120	0—5	63
	25	0.03[f]	110	0—5	63
^{35}ClF					
	5	0.029	*s*	16	85

[a] The data presented in this table are the result of a critical evaluation of the measurements made by direct observation of fluorescence decay. Where the decay rates show a linear dependence on the rotational energy they are represented by the expression:

$$\Gamma = \Gamma_{00} + k_{v'} J'(J' + 1)$$

The extensive data for I_2 (B) have not been considered in this review. Summaries of these results are given in references 4 and 5. [b] The decay rates for $I^{35}Cl(B)$, $v' = 3$ show a complex dependence on J'. See references 27 and 29 for details. [c] IF (B) $v' = 9$ levels with $7 \leq J' \leq 41$ show a constant decay rate of $9.1 \times 10^5 s^{-1}$. [d] For $Br_2(B)$, $5 \leq v' \leq 24$ the Γ_{00} values are poorly determined by extrapolation of the data for predissociated levels. The estimates given here have been calculated using the transition moment function of LeRoy *et al.*[39] [e] The decay rates for $Br_2(B)$, $v' = 7$ show a complex dependence on J' and isotopic composition. See Figure 15. [f] For $^{35}Cl_2(B)$, $13 \leq v' \leq 25$ the Γ_{00} values are poorly determined by extrapolation of the data for predissociated levels. The $k_{v'}$ values given here have been determined by fixing Γ_{00} to the radiative rate measured for $v' = 5$. [g] Levels which are stable with respect to predissociation

shortest lifetimes. This trend is illustrated in Table 1, where the radiative lifetime data are roughly correlated with the spin–orbit coupling and the molecular mass. A more detailed summary of the collision-free fluorescence decay data discussed in this review is given in Table 2.

From a practical standpoint lifetime measurements become more difficult as the lifetime increases. The low pressure needed for collision-free observation, coupled with the inherent weakness in fluorescence of a long-lived transition, results in a very low signal intensity. Diffusion of the excited molecules becomes a problem because of the large mean free paths between collisions. When collisions do not occur the decay dynamics are frequently modified by rotational and vibrational energy transfer. Therefore, in presenting the results of the fluorescence decay studies I will progress from short to long lived states, so that the complications arising from non-radiative decay, collisional energy transfer, and diffusion are encountered sequentially.

A. Iodine Monobromide.—The appropriate wavelength range for recording an excitation spectrum is defined by the positions of the strongest absorption bands

which terminate on stable excited-state levels. If the frequency dependence of the transition probability is ignored, the absorbance of a particular band is directly proportional to the product of the fractional population in the ground-state level and the Franck–Condon factor, *i.e.*,

$$A \propto q_{v',v''} \frac{N_v}{N_{\text{total}}}$$

The absorption spectrum for the IBr *B*—*X* system is well known,[1] and it is evident that levels with $v' \geqslant 5$ are unstable and therefore will not be active in the excitation spectrum (*cf.* Figure 4). The Franck–Condon factors connecting the levels $v' \leqslant 4$ with the ground state favour transitions from vibrationally excited ground-state levels.[21] For example, the relative absorption strengths for the progression of bands terminating on $v' = 3$ are given in Table 3, where it can be seen that the absorptions from $3 \leqslant v'' \leqslant 5$ are best for exciting the $v' = 3$ level. Once the bands most suited for observation by LIF have been identified, a search for the excitation spectrum can be made using a variety of different pressure and composition conditions.

Table 3 *Vibrational populations, Franck–Condon factors, and relative absorption strengths for* $I^{79}Br$, *B–X*, 3,v'' *transitions*

v''	$\frac{N_{v''}}{N}$	$q_{3,v''} \times 10^4$	$\frac{q_{3,v''} N_{v''} \times 10^6}{N}$
0	0.727	0.01	0.7
1	0.197	0.2	3.9
2	0.0545	1.7	9.3
3	0.0154	9.0	14
4	0.0042	34.4	14
5	0.0012	99.6	12

Initial attempts to record LIF from the IBr *B*—*X* system failed because the signals were swamped by the fluorescence emitted by the small amounts of I_2 present in the sample.[22] The I_2 originated from the equilibrium $2IBr \rightleftharpoons I_2 + Br_2$, and it was effectively suppressed by adding excess Br_2 to the IBr sample.[21] The presence of excess Br_2 drove the equilibrium towards IBr, but did not interfere with the observation of the IBr spectrum. Figure 7 shows an example of the IBr (*B*—*X*) excitation spectrum. The rotational structure in this trace is almost fully resolved, and the lines belonging to the two isotopic species ($I^{79}Br$ and $I^{81}Br$) are readily differentiated. This spectrum is quite dense, but straightforward in its underlying structure. The rotational selection rules for a 0^+—0^+ transition are $\Delta J = +1$ (*R*-branch) and $\Delta J = -1$ (*P*-branch). By convention the lines are numbered according to their ground state *J* values. When the lines are assigned it becomes

[21] M. A. A. Clyne and M. C. Heaven, *J. Chem. Soc., Faraday Trans. 2*, 1980, **76**, 49.
[22] M. A. A. Clyne and I. S. McDermid, *J. Chem. Soc., Faraday Trans. 2*, 1976, **72**, 2252.

apparent that the intensity distribution does not reflect a Boltzmann distribution of population among the ground-state rotational levels. At thermal equilibrium the maximum in the population distribution occurs at $J'' = 45$, and levels up to $J'' = 100$ contain significant population. In contrast, the maximum intensity in Figure 7 occurs for lines originating from $J'' \approx 10$, and lines from $J'' > 64$ could not be detected. This anomalous rotational distribution indicated the presence of a non-radiative decay channel, the nature of which is explained below in terms of a rotationally dependent predissociation.

LIF spectra for the 2—2 and 2—3 vibronic bands were recorded,[21] and these also showed anomalous distributions of rotational line intensities. Bands terminating on $v' = 4$ (4—3 and 4—4) were predicted to be more intense than the 3—3 band, but these could not be seen. This suggests that the predissociation for $v' = 4$ must be at least 20 times faster than it is for $v' = 3$ (a limit set by the noise level in the spectrum). Prior to these experiments, predissociation in levels with $v' \leqslant 4$ had not been detected because the predissociation has to be severe to cause perceptible line broadening in the absorption spectrum.

Further details of the predissociation were revealed by recording fluorescence decay lifetimes for isolated ro-vibrational levels of the $v' = 2$ and 3 manifolds.[21] Measurements were made over the pressure range from 1 to 5 mtorr. Within this range the decay curves were unaffected by pressure, and the longest lifetime measured was 350 ns. The absence of collisional effects was not surprising, as at 5 mtorr the average time between collisions is 18 μs. For both vibrational manifolds the fluorescence decay rate increased with the rotational energy, and for a fixed value of J' the lifetimes of the $v' = 3$ levels were always shorter than those for $v' = 2$. The range of τ_0 for $v' = 2$ of $I^{81}Br$ was from 290 ns for $J' = 7$ to 70 ns for $J' = 34$. For $v' = 3$ of $I^{81}Br$, τ_0 varied from 72 ns at $J' = 3$ to 28 ns at $J' = 32$. Examples of the fluorescence decay curves are shown in Figure 8, where the effect of vibrational energy on the lifetime is easily seen.

The rotational dependence of the IBr lifetimes is a consequence of a heterogeneous predissociation ($\Delta\Omega = 1$). Rotational motion mixes the bound and repulsive states, resulting in a first-order rate constant for predissociation which depends on J' according to [13,23]

$$\Gamma_p = k_{v'} J'(J' + 1) \tag{4}$$

where $k_{v'}$ is a constant for a given vibrational level (with exceptions which are discussed in the section on Br_2). Thus the collision-free lifetime τ_0 is determined by the relationship:

$$1/\tau_0 = 1/\tau_{00} + k_{v'} J'(J' + 1) \tag{5}$$

If the predissociation is exclusively heterogeneous, the lifetime for the rotationless level ($J' = 0$) is equivalent to the purely radiative lifetime τ_r. Figure 9 shows the decay rates for the $v' = 3$ levels plotted against $J'(J' + 1)$, where the data give reasonably good fits to equation 5. There is a slight, but significant, difference

[23] J. T. Hougen, 'Calculation of Rotational Energy Levels and Rotational Line Intensities in Diatomic Molecules', NBS Monograph No. 115.

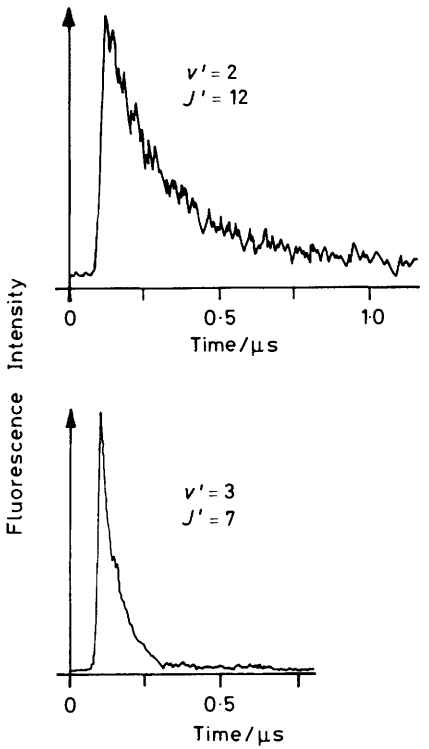

Figure 8 *Typical fluorescence decay curves for* IBr(*B*). *Decay curves are shown for the* (2,12) *and* (3,7) *ro-vibrational states of* $I^{81}Br$. *Note the much shorter lifetime of the* $v' = 3$ *state* (Reproduced by permission from *J. Chem. Soc., Faraday Trans. 2*, 1978, **76**, 49)

between the data sets for the two isotopes. Decay rates for the $v' = 2$ manifold also gave a reasonable fit to equation 5, but for this state only one isotope was studied ($I^{81}Br$). Analysis of the lifetime data yielded the following parameters:

$v' = 2$ of $I^{81}Br$:	$\tau_{00} = 440$ ns, $k_{2'} = 1.1 \times 10^4$ s^{-1}
$v' = 3$ of $I^{81}Br$:	$\tau_{00} = 70$ ns, $k_{3'} = 2.1 \times 10^4$ s^{-1}
$v' = 3$ of $I^{79}Br$:	$\tau_{00} = 62$ ns, $k_{3'} = 2.8 \times 10^4$ s^{-1}

The difference in τ_{00} between $v' = 2$ and $v' = 3$ is much too large to be explained in terms of changes in $|R_e|^2$ or $(\bar{\nu})^3$. Hence, there must be predissociation of the rotationless levels in $v' = 3$ caused by a homogeneous interaction. Clearly, Figure 9 could not be used to determine τ_r, so the question of whether $v' = 2$, $J' = 0$ was also predissociated became of importance. To clarify this question, an estimation of τ_r was made by calculating $A_{v'}$. Extended Franck–Condon calculations were performed to determine $(\bar{\nu})^3$, with $|R_e|^2$ assumed to be 0.7 D^2, the mean of the values for I_2 (1.0 D^2) and Br_2 (0.4 D^2). For $v' = 2$ this procedure predicted a lifetime of 4 ± 2 μs, a factor of 9 greater than the corresponding τ_{00} value. Thus the measured

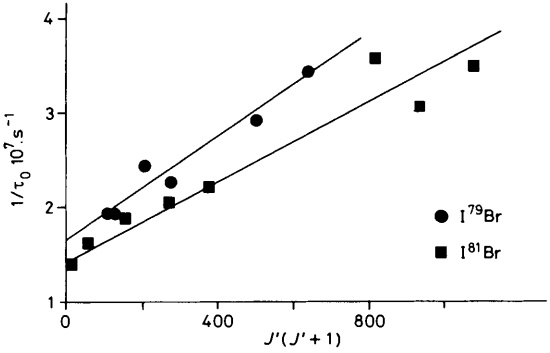

Figure 9 *Fluorescence decay rates for* IBr(*B*). *Plots of* $1/\tau_0$ *against* $J'(J+1)$ *for the* $v' = 3$ *rotational manifolds of* ●, $I^{79}Br(B)$, *and* ■, $I^{81}Br(B)$
(Reproduced by permission from *J. Chem. Soc., Faraday Trans. 2*, 1978, **76**, 49)

rotation-free lifetimes were strongly influenced by homogeneous predissociation.

The *B* states of I_2, Br_2, and ICl all suffer heterogeneous predissociation caused by interaction with the repulsive 2431 $^1\Pi$ (1) state (see below). Arguing by analogy, it is most likely that the heterogeneous component of the IBr(*B*) predissociation is also caused by the interaction with $^1\Pi$ (1). The $Y(0^+)$ state, which causes the avoided crossing, is probably also the state which is responsible for the homogeneous component of the predissociation. Levels lying at energies below the crossing point dissociate by tunnelling through the potential energy barrier. The probablity for this process decreases as the separation between the vibrational level and crossing point increases, so the fact that the predissociation for $v' = 2$ is weaker than it is for $v' = 3$ is readily understood. Similarly, the vibrational energy of $I^{79}Br$ $v' = 3$ is slightly higher than $I^{81}Br$ $v' = 3$, and the former is more rapidly predissociated. The absence of detectable fluorescence from $v' = 4$, and the strength of the predissociation in $v' = 3$, suggests that the energy of the curve crossing shown in Figure 4 may be too high, but further theoretical calculations of the tunnelling probabilities are required to investigate this possibility.

The radiative lifetime for IBr(*B*) $v' = 0$, isolated in an argon matrix at 12K, has recently been measured by Nicolai and Heaven.[24] They obtained a value of 0.73 μs, which, after correction for the refractive index of the matrix, is equivalent to a gas-phase lifetime of 1.4 μs. Thus the foregoing conclusions concerning homogeneous predissociation of $v' = 2$ are confirmed.

B. Iodine Monochloride.—The *B* states of ICl and IBr are very similar in their general characteristics. As for IBr(*B*), the *B* state of ICl forms an avoided crossing with the repulsive $Y(0^+)$ state, and the *B*—*X* absorption spectrum [1] shows only fragmentary and erratic structure for levels with $v' > 3$. The Franck–Condon

[24] J. P. Nicolai and M. C. Heaven, to be published.

factors[25] connecting levels with $v' \leqslant 3$ to the ground state are very small for $v'' = 0$, and these levels are more efficiently populated from vibrationally excited ground-state levels. At room temperature the low population in these levels leads to a weak absorption, and the *B*—*X* system is heavily overlapped by the *A*—*X* system. Despite the smaller dipole moment for the *A*—*X* transition, these bands appear to be as intense as the *B*—*X* bands because they originate from $v'' = 0$ with large Franck–Condon factors. (Overlapping of the *B*—*X* and *A*—*X* systems of IBr is not seen because the *B* and *A* states are widely separated by the strong spin–orbit coupling).

The optimum spectral region for observing the laser excitation spectrum of the ICl *B*—*X* system is between 600 and 620 nm. Within this range Clyne and McDermid[22] obtained a very congested spectrum from a commercial sample of ICl (0.1 torr ICl in 2 torr He). On analysis it was found that the spectrum consisted of overlapping bands from ICl(*A*—*X*), ICl(*B*—*X*), and I_2(*B*—*X*). Fluorescence from ICl(*A*) and I_2(*B*) could be effectively suppressed by increasing the ICl pressure. Spectra dominated by the ICl *B*—*X* system were recorded at a total pressure of 5 torr. (This experiment illustrates one of the valuable aspects of the LIF technique. The fluorescence decay kinetics can often be manipulated to separate overlapping electronic transitions.)

Suppression of the *A*—*X* system allowed Clyne and McDermid[22] to observe transitions to the *B* state $v' = 0$ level for the first time. Rotationally resolved spectra for the 0—2 band were analysed and used to determine the rotational constant (B'_0) and the origin of the band system. This information was combined with the results from the absorption studies to provide improved parameters for the polynomial representations for the vibrational energy and rotational constants.

Fluorescence from transitions terminating on $v' = 3$ could not be seen due to predissociation. Lifetime measurements[26] were made for various rotational levels of $v' = 2$ and 1, but the 0—2 band was too weak for measurement of the $v' = 0$ lifetime. Collision-free conditions could not be used in this work. The low power of the excitation laser necessitated the use of fairly high ICl pressures (> 0.2 torr), and the zero pressure lifetimes were determined by extrapolation of the Stern-Volmer plots (which were linear in the range $0.2 < p_{ICl} < 1.5$ torr). The lifetime appeared to be independent of vibrational and rotational energy for $v' = 1$ and 2. An average value of 0.52 μs was found, and the rate constant for self deactivation was near gas kinetic (2.1×10^{-10} cm^3 molecule^{-1} s^{-1}). Subsequent work has shown that extrapolation of the Stern–Volmer plots was not a valid procedure. Kitamura *et al.*[27] have measured the lifetime for $v' = 1$ at pressures as low as 10 mtorr. They found a value of 4.1 μs, in good agreement with the results from a study[28] of matrix isolated ICl ($\tau_{gas} = 4.6$ μs, after correction for the refractive index of the matrix host). This implies that the self quenching Stern–Volmer plots are curved in the region between 0 and 0.2 torr. Such curvature would not be surprising, as

[25] M. A. A. Clyne and I. S. McDermid, *J. Chem. Soc., Faraday Trans. 2*, 1976, **72**, 2242.
[26] M. A. A. Clyne and I. S. McDermid, *J. Chem. Soc., Faraday Trans. 2*, 1977, **73**, 1094.
[27] M. Kitamura, T. Kondow, and K. Kuchitsu, *J. Chem. Phys.*, 1985, **82**, 4986.
[28] V. E. Bondybey and L. E. Brus, *J. Chem. Phys.*, 1975, **62**, 620.

vibrational energy transfer to unstable levels may well compete with electronic quenching at these pressures.

Rotationally dependent predissociations have been seen in the $v' = 2$ and 3 manifolds.[27,29] The predissociation of $v' = 2$ is a purely heterogeneous process, while $v' = 3$ appears to be influenced by both homogeneous and heterogeneous interactions.[29]

C. Iodine Monofluoride.—Conventional absorption spectra for the IF(B—X) system have never been recorded, and this transition is known primarily from the emission spectrum resulting from the $I_2 + F_2$ reaction.[30] The emission data show that the low-lying electronic structure of IF is somewhat different from that of IBr and ICl. As noted previously, the interhalogen B states correlate with one of two possible combinations of a ground-state atom and a spin–orbit excited atom. IBr(B) and ICl(B) correlate with the lower energy combination ($I\ ^2P_{\frac{3}{2}} + Br\ ^2P_{\frac{1}{2}}$ and $I\ ^2P_{\frac{3}{2}} + Cl\ ^2P_{\frac{1}{2}}$), whereas IF($B$) correlates with the higher energy limit ($I\ ^2P_{\frac{1}{2}} + F\ ^2P_{\frac{3}{2}}$). The IF B state is tightly bound, with its potential energy curve dipping well below the ground state dissociation limit.[31] Above this limit the B state is predissociated by a partially avoided crossing with the $Y(0^+)$ state, and emission for levels with $v' = 11$ could not be seen. The displacement between the equilibrium internuclear separations for the X and B states is small, and as a consequence transitions from $v'' = 0$ to stable levels of the B state ($3 \leqslant v' \leqslant 8$) have large Franck–Condon factors.[25] These properties make IF an ideal species for detection by LIF. The potential energy curves which are relevant to the present discussion are shown in Figure 10.

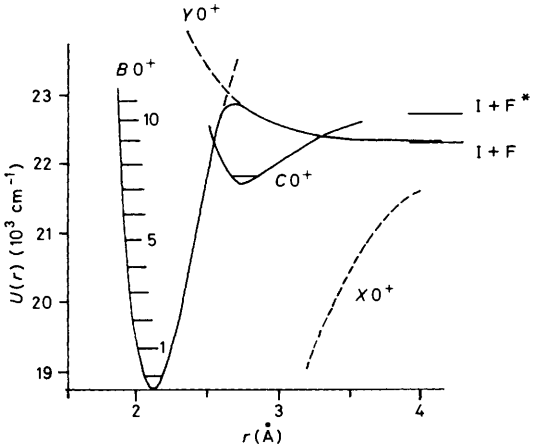

Figure 10 *Potential energy curves for the low-lying* 0^+ *states of* IF
(Reproduced by permission from *J. Chem. Soc., Faraday Trans. 2*, 1978, **74**, 1644)

[29] T. Suzuki and T. Kasuya, *J. Chem. Phys.*, 1984, **81**, 4818.
[30] R. A. Durie, *Can. J. Phys.*, 1966, **44**, 337.
[31] J. A. Coxon, *Chem. Phys. Lett.*, 1975, **33**, 136.

Preliminary laser excitation spectra for the IF B—X system were recorded in a simple flow tube apparatus. Clyne and McDermid[22] generated IF by the reaction $F + ICl \longrightarrow IF + Cl$ in the presence of a large flow of He carrier gas. Intense fluorescence was observed from levels with $v' \leqslant 9$. The large vibrational and rotational spacings in the ground state, dominance of the $v'' = 0$ progression, and the existence of only one isotopic molecule ($^{127}I^{19}F$) result in a beautifully simple excitation spectrum. Figure 11 shows the origin band (0—0), which is a comparatively weak transition that has only been observed by LIF techniques.[32] The flow tube studies[22] gave evidence for predissociation in the $v' = 10$ level, where the rotational intensity distribution was markedly non-Boltzmann. Predissociation was not seen in this level in the earlier emission studies, presumably because the predissociation rate was not fast enough to compete with collisional deactivation in the high pressure flames. The lower energy onset of predissociation seen in the LIF spectrum provided an improved upper limit for the ground-state dissociation limit ($D_0 \leqslant 22\,700$ cm^{-1}).

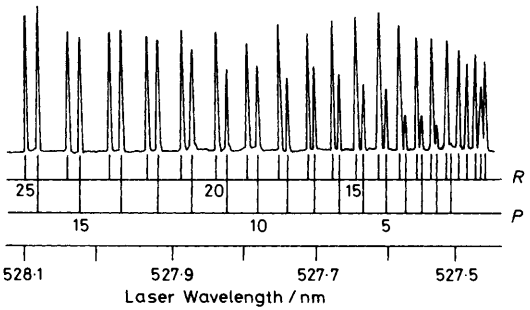

Figure 11 *Laser excitation spectrum of the* 0—0 *band of the IF B—X system. This is the weakest of the* IF *bands with a Franck–Condon factor of* 4.8×10^{-3} (Reproduced by permission from *J. Chem. Soc., Faraday Trans. 2*, 1978, **74**, 1644)

Attempts to determine the radiative lifetime of the B state were hampered by difficulties in maintaining the IF concentration when the flow conditions were changed.[26] In a later study, Clyne and McDermid[32] used the apparatus described previously (*cf.* Figure 6) to record spectra and lifetimes at total pressures less than 1 mtorr. At such low pressures it was possible to observe the onset of predissociation within the rotational manifolds of $v' = 8$ and 9. As shown in Figure 12, the onset of predissociation at $v' = 9$, $J' = 7$ was immediately obvious in the 9—0 band. Lifetime measurements confirmed that the intensity anomalies were caused by predissociation. Levels within the range $0 \leqslant v' \leqslant 7$ were found to be entirely stable, with lifetimes ranging from 7.0 μs for $v' = 0$ to 8.6 μs for $v' = 7$. The electronic transition moments for the stable levels, calculated from the lifetime data by use of equation 2, were almost independent of the vibrational state ($|R_e|^2 = 0.10 \pm 0.01\ D^2$). Thus the slight vibrational dependence of the lifetime

[32] M. A. A. Clyne and I. S. McDermid, *J. Chem. Soc., Faraday Trans. 2*, 1978, **74**, 1644.

stems from the $(\nu)^3$ factor. The lifetime within the $v' = 8$ manifold was unaffected by predissociation for $J' \leqslant 49$, but the value dropped from 8.0 μs for $J' = 50$ to 2.4 μs for $J' = 54$ (the fluorescence from levels with $J' > 54$ was undetectably weak). Some care was needed in assigning the first level *directly* affected by predissociation. Although the lifetime for $J' = 50$ was 10% smaller than the average value for the preceding levels, it was argued that this state was probably deactivated by efficient energy transfer to genuinely unstable levels. With the assumption of a gas kinetic energy transfer rate it was concluded that predissociation first occurred at $v' = 8$, $J' = 52$. The onset of predissociation in $v' = 9$ was sharp, occurring at $J' = 7$, and the lifetimes dropped from 8.1 μs for $J' = 6$ down to 1.1 μs for $7 \leqslant J' \leqslant 41$. There were no stable levels of $v' = 10$, and the lifetime decreased smoothly from 0.44 μs at $J' = 0$ to 0.33 μs at $J' = 21$.

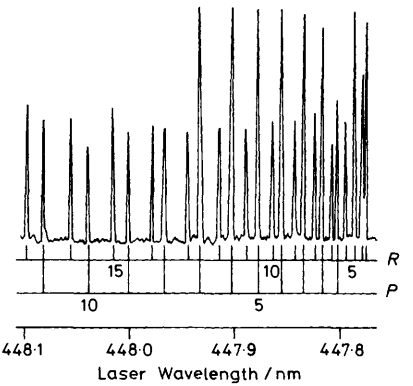

Figure 12 *Laser excitation spectrum of the* 9—0 *band of the* IF *B—X system. Note the anomalously weak rotational lines for transitions with* $J' > 7$
(Reproduced by permission from *J. Chem. Soc., Faraday Trans. 2*, 1978, **74**, 1644)

Analysis of the predissociation threshold energies provided both an improved estimate for the ground-state dissociation limit, and information about the dissociative state involved. The $v' = 8$, $J' = 52$ level is at an energy which is 225.3 cm^{-1} above the $v' = 9$, $J' = 7$ level, and this difference reflects the height of the rotational barrier to dissociation.[9] The internuclear distance corresponding to the maximum of this barrier, determined from the energy spacing, was $r = 3.5$ Å. If the state causing dissociation is entirely repulsive the position of the maximum will be close to the r value of the curve crossing. From Figure 10 it is clear that this is not the case for $v' = 8$ and 9, and the dissociative state must be bound at lower energies [Herzberg's case I(b)]. Clyne and McDermid[32] tentatively assigned the dissociation to the weakly bound $C(0^+)$ state, which correlates diabatically with the $I\ ^2P_{\frac{3}{2}} + F\ ^2P_{\frac{1}{2}}$ atomic products. At first sight it would appear that the predissociation threshold defines the energy of this dissociation limit with respect to $v'' = 0$ (*i.e.* $D_0'' + E(F\ ^2P_{\frac{1}{2}})$). However, $C(0^+)$ is itself predissociated by an interaction with the $Y(0^+)$ state, and the threshold actually corresponds to the

ground-state dissociation limit. After correction for the rotational barrier, a value of $D_0' = 22\,333 \pm 2\text{cm}^{-1}$ was obtained.

The lifetime behaviour of the entire $v' = 8$ and 9 rotational manifolds can be rationalized in terms of the *B*—*C* interaction. Immediately above threshold, the predissociation in the $v' = 8$ levels is very rapid, indicating a reasonably good Franck–Condon overlap between *B*, $v' = 8$ and the *C* state continuum. The short but constant lifetime of the $v' = 9$, $J' > 6$ levels is consistent with a homogeneous predissociation, although the Franck–Condon overlap between *B*, $v = 9$ and the continuum must be much smaller than for $v' = 8$ (this is physically reasonable as the Franck–Condon densities for bound—free transitions often show an oscillating dependence on v'[13,14]). Interpretation of the rotationally dependent lifetime data for $v' = 10$ is more difficult. The decay rate does increase linearly with the rotational energy, suggesting a heterogeneous interaction, but the evident predissociation of $v' = 10$, $J' = 0$ requires a competing homogeneous channel. Alternatively the predissociation may be exclusively homogeneous, with the rotational dependence arising from the subtle influence of the rotational motion on the Franck–Condon densities. Given the available data, it is impossible to distinguish between these two mechanisms.

D. Bromine.—From a spectroscopic standpoint, the Br_2 *B*—*X* transition has been characterized in great detail.[1] Although the bands of this transition have a simple *P* and *R* branch structure, the low magnitudes of the vibrational and rotational constants give rise to an extremely overlapped and dense spectrum. The complexity is compounded by the natural occurrence of three isotopes $^{79}Br_2$, $^{79}Br\,^{81}Br$, and $^{81}Br_2$ in the approximate ratio 1:2:1. Other low lying electronic transitions known for Br_2 include the *A*—*X* system and the $^1\Pi$ (1_u) continuum absorption.[1] Some of the experimentally determined potential energy curves for Br_2 are shown in Figure 3.

Estimates for the *B* state lifetime, derived from studies of matrix-isolated[33] Br_2 and absorption coefficient measurements,[1] were in the range of 10 to 25 μs. Several early attempts to measure the radiative lifetime in the gas phase were made using pulsed laser excitation.[1,5] Values ranging between 3.57—0.11 μs were observed at differing energies within the *B* state. The variability and shortness of these lifetimes provided adequate evidence of a quantum state dependent predissociation, but the fragmentary nature and large uncertainties of the early studies did not allow for quantitative characterization of this process.

Systematic studies of the *B*—*X* system laser excitation spectrum, and measurements of the *B* state lifetime as a function of v' and J', were made by Clyne and Heaven.[34] Excitation spectra, recorded at pressures of 10 mtorr or less, showed the non-Boltzmann intensity distributions which are characteristic of a state-dependent predissociation. The intensity maxima in all bands with $v' > 10$ appeared at J' values considerably lower than those predicted by theory or seen in absorption spectra. Lifetime measurements[34] confirmed that these anomalies were

[33] V. E. Bondybey, S. S. Bearder, and C. Fletcher, *J. Chem. Phys.*, 1976, **64**, 5243.
[34] M. A. A. Clyne and M. C. Heaven, *J. Chem. Soc., Faraday Trans. 2*, 1978, **74**, 1992.

caused by a rotationally dependent predissociation. Within each vibrational state the fluorescence decay rates were found to be linearly dependent on $J'(J' + 1)$ as illustrated in Figure 13 for $v' = 11$ and 14. The lifetimes were, however, independent of the isotopic species (except for $v' = 7$) and, for the symmetric isotopes, of the *ortho–para* symmetry. For vibrational levels in the range $4 \leqslant v' \leqslant 25$ the data gave excellent fits to the heterogeneous predissociation expression (equation 5). The rotation-free lifetimes were determined by extrapolations based on equation 5. This procedure produced rather scattered results, but the mean value (8.1 μs) was close to the expected radiative lifetime. As for $I_2(B)$ and $Cl_2(B)$ (see below) the predissociation of $Br_2(B)$ is exclusively heterogeneous.

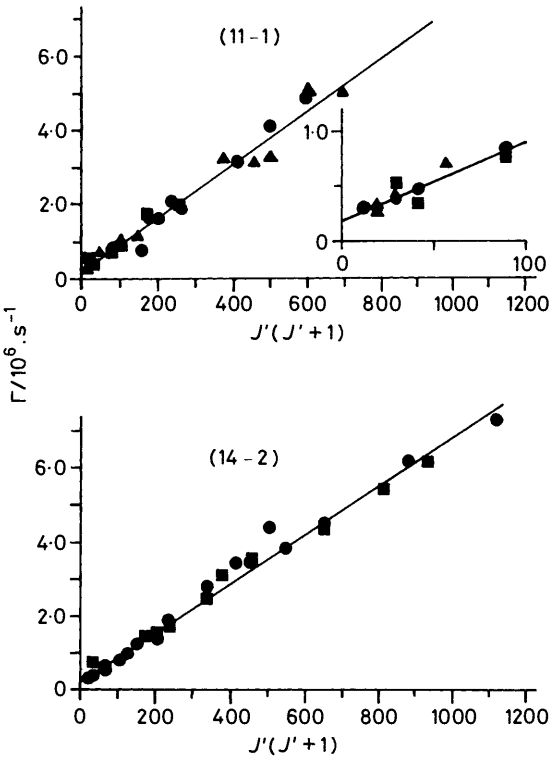

Figure 13 *Fluorescence decay rates for* $Br_2(B)$. *Plots of* Γ *against* $J'(J' + 1)$ *for the rotational manifolds of* $v' = 11$ *and* 14. ▲, $^{79}Br_2$; ■, $^{81}Br_2$; ●, $^{79}Br^{81}Br$
(Reproduced by permission from *J. Chem. Soc., Faraday Trans. 2*, 1978, **74**, 1992)

The predissociation rate constants, $k_{v'}$, determined from the slopes of the decay rate *vs.* $J'(J' + 1)$ plots, are also quantum state dependent as shown in Figure 14.

The $k_{v'}$ values are proportional to the vibrational wavefunction overlap integrals. Theoretical treatments yield the approximate relationship,

$$k_{v'} = k^* | \langle X_c | r^{-2} | X_b \rangle |^2 \quad (6)$$

where k^* is a constant and X_c and X_b are the continuum and bound state vibrational wavefunctions, respectively. Accurate vibrational wavefunctions for the *B* state can be generated from the potential energy curve, and used in equation 6 to obtain information about the repulsive potential *via* trial-and-error Franck–Condon calculations. Clyne, Heaven, and Tellinghuisen[35] used this approach to characterize the repulsive state over the range of internuclear separation spanned by the lifetime data ($2.5 \leqslant r \leqslant 3.1$ Å). Child[36] has also analysed the $k_{v'}$ pattern to determine the repulsive potential. Using a purely analytical method he obtained a potential which was in excellent agreement with the results of the more laborious Franck–Condon calculations.

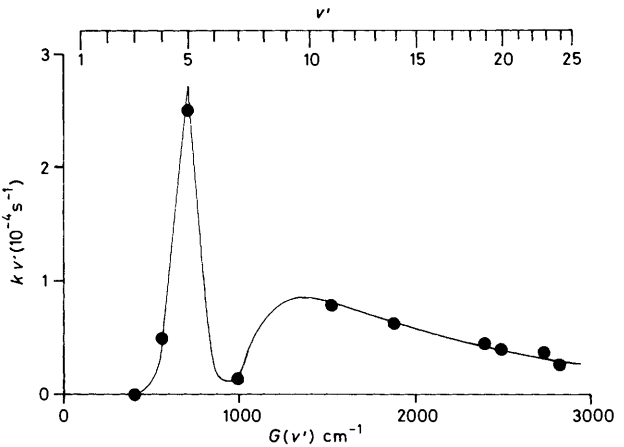

Figure 14 $Br_2(B)$ *predissociation rate constants,* $k_{v'}$*, as a function of the vibrational energy. The filled circles represent the experimental data, and the smooth curve shows the results from Franck–Condon density calculations*
(Reproduced by permission from *J. Chem. Phys.*, 1982, **76**, 5341)

The vibrational wavefunctions in equation 6 are implicitly dependent on the angular momentum and isotopic composition. However, when the overlap integral is large the predissociation probabilities are not significantly influenced by these factors. This is the case for all of the vibrational levels studied, with the exception of $v' = 7$. For this level the phase relationships between the bound and continuum wavefunctions are such that they suffer destructive interference, and the predissociation probability is very low.[35] Small changes in the phase relationships,

[35] M. A. A. Clyne, M. C. Heaven, and J. Tellinghuisen, *J. Chem. Phys.*, 1982, **76**, 5341.
[36] M. S. Child, *J. Phys. B: At. Mol. Phys.*, 1980, **13**, 2557.

produced by the rotational energy or by isotopic substitution, result in large changes in the final integral. Figure 15 shows the decay rates for $v' = 7$ plotted against $J'(J' + 1)$. The linear correlation is lost because $k_{v'}$ is now also a function of J'. In addition, the isotopic dependence of $k_{v'}$ is clearly demonstrated. This interesting behaviour was first noticed in the Franck–Condon calculations, and then quantitatively verified by experiment.[37]

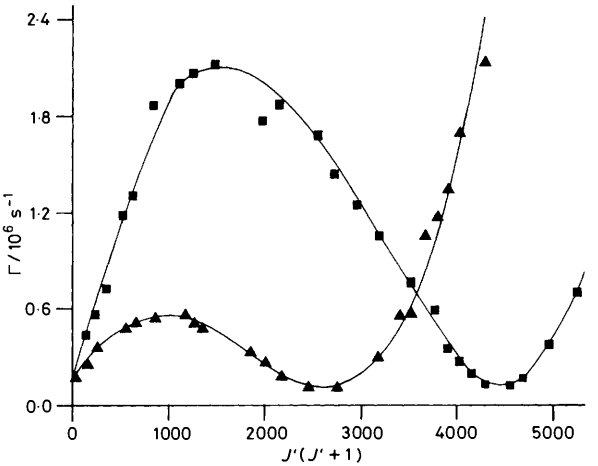

Figure 15 *Fluorescence decay rates for* $Br_2(B)$. Plots of Γ *against* $J(J' + 1)$ *for the* $v' = 7$ *rotational manifold* ▲, $^{79}Br_2$; ■, $^{81}Br_2$

All vibrational levels of the B state with $v' > 0$ lie above the ground state dissociation limit, and are therefore capable of predissociation. The $^1\Pi$ (1_u) state crosses the B state between $v' = 4$ and $v' = 5$, strongly destabilizing the latter. Levels at energies below the crossing point predissociate by tunnelling, but the probability of this event falls rapidly with decreasing energy. The Franck–Condon calculations predict a negligible probability for predissociation of $v' = 2$, which makes this level ideal for measurement of the radiative lifetime (absorptions to $v' = 0$ and 1 were too weak to be used for this purpose). Clyne, Heaven, and Martinez[38] measured the collision-free lifetimes for selected $v' = 2$ levels in the range $4 \leqslant J' \leqslant 31$. The lifetime was independent of the rotational state, with an average value of 12.4 μs. Calculation of the transition dipole moment from the lifetime is difficult for the Br_2 B—X transition because $|R_e|^2$ is known to vary significantly with $\bar{r}$. From an analysis of the B—X continuum absorption spectrum, Le Roy *et al.*[39] have derived a function which characterizes this dependence. This equation was evaluated by its use in equation 1 to determine the radiative lifetime. The value obtained, 11.3 ± 1.0 μs, was in remarkable agreement with the direct measurement,

[37] M. A. A. Clyne, M. C. Heaven, J. Maliekal, and E. Martinez, to be published.
[38] M. A. A. Clyne, M. C. Heaven, and E. Martinez, *J. Chem. Soc., Faraday Trans. 2*, 1980, **76**, 405.
[39] R. J. LeRoy, R. G. Macdonald, and G. Burns, *J. Chem. Phys.*, 1976, **65**, 1485.

in view of the totally dissimilar methods on which the two determinations were based.

The measurement of quenching rate constants for the *B* state is complicated by the ro-vibrational level dependence of the lifetime. In a study of the $v' = 11$ and 14 levels, Clyne, Heaven, and Davis[40] found that self and foreign gas quenching rate constants, determined by the usual Stern–Volmer analysis, showed an apparent dependence on the rotational energy of the initially excited level. In addition, quenching plots associated with initial excitation of low J' levels ($J' < 10$) exhibited a marked negative curvature. Both of these characteristics were interpreted in terms of a deactivation mechanism involving fast energy-transfer to strongly predissociated levels. Self-deactivation rate constants in the range of 4.1—9.2 $\times$ 10^{-10} cm^3 $molecule^{-1}$ s^{-1} were reported, and it was argued that the lower values reflected the true electronic quenching efficiency. Wavelength-resolved fluorescence spectra were recorded in an attempt to observe emission from collisionally populated states, but for $Br_2(B) + Br_2(X)$ collisions this was not feasible as the kinetics were dominated by quenching. Much lower electronic quenching rate constants were found for Ar and N_2. With these collision partners the fluorescence from collisionally populated ro-vibrational states could be observed, and used to provide estimates of the energy-transfer rate constants. Ar proved to be effective as a rotational energy-transfer agent [$k(Ar,R—T) \approx 4 \times 10^{-11}$ cm^3 $molecule^{-1}$ s^{-1}], while N_2 promoted vibrational energy relaxation [$k(N_2,v—v) \approx 2.5$ 10^{-11} cm^3 $molecule^{-1}$ s^{-1}].

Electronic quenching of $Br_2(B)$ is primarily caused by collision-induced predissociation,

$$Br_2(B) + M \longrightarrow Br + Br + M$$

This process depends on the collisional mixing of the *B* state with a nearby continuum state, and the extent of mixing (and therefore the quenching rate constant) is governed by the Franck–Condon principle. Thus the quenching rate constant may also be expected to depend on the vibrational state. Although the data are limited, such a dependence has been clearly observed in the self-quenching studies. There is an almost order-of-magnitude drop in the rate constant in going from the $v' = 11$ and 14 levels[40] to the $v' = 2$ level[38] [$k_q(v' = 2) = 5.8 \times 10^{-11}$ cm^3 $molecule^{-1}$ s^{-1}].

The *A*—*X* and *B*—*X* systems of Br_2 are well separated, and at wavelengths greater than 650 nm the *A*—*X* system dominates the absorption spectrum. Clyne, Heaven, and Martinez[41] investigated the laser excitation spectrum of Br_2 in the wavelength region of 690 to 710 nm, where they found dense, but rotationally resolved, structure belonging to the *A*—*X* system. Measurement of the fluorescence decay lifetime for the *A* state proved to be a difficult undertaking. The long lifetime ($> 100\mu s$) necessitated the use of pressures below 1 mtorr, and extensive signal averaging was required to obtain usable signal-to-noise ratios. Diffusional

[40] M. A. A. Clyne, M. C. Heaven, and S. J. Davis, *J. Chem. Soc., Faraday Trans. 2*, 1980, **76**, 961.
[41] M. A. A. Clyne, M. C. Heaven, and E. Martinez, *J. Chem. Soc., Faraday Trans. 2*, 1980, **76**, 177.

distortion of the fluorescence decay curves was also a problem in this work. Owing to the weakness of the fluorescence, this could not be alleviated by moving the detector away from the laser axis. Instead the effects of the distortion were avoided by determining the lifetime from the first 200 μs of the decay, as this period corresponded to an acceptably small diffusion radius. Even with these precautions, collision-free measurement could not be achieved, and a radiative lifetime of 350 ± 50 μs ($v' = 11$) was determined from a short Stern–Volmer extrapolation. The apparent self-deactivation rate constant defined by the Stern–Volmer plot was surprisingly large ($k_q = 2.4 \times 10^{-10}$ cm^3 molecule^{-1} s^{-1}), and inconsistent with the known recombination afterglow kinetics.[42] However, when the lifetime measurements were repeated with a different photomultiplier tube (one with a higher quantum efficiency at long wavelengths), the apparent rate constant fell to 8.0×10^{-11} cm^3 molecule^{-1} s^{-1}. Analysis of these experiments, and of the non-exponential decay curves seen at high pressures (> 50 mtorr), lead to the conclusion that vibrational energy transfer was responsible for the apparent deactivation (*cf.* equation 4 and the accompanying discussion). The true electronic self-quenching rate constant was too small to be measured in this work ($< 5 \times 10^{-12}$ cm^3 molecule^{-1} s^{-1}). so the deactivation rate constant of 2.4×10^{-10} cm^3 molecule^{-1} s^{-1} must set a lower limit for the vibrational relaxation process.

E. Bromine Monochloride.—Consideration of the data for the other halogens and interhalogens suggests that the *B*—*X* transition for BrCl should be about four times weaker then $Br_2(B—X)$. Experimentally the absorption spectrum was found to be extremely weak, and the *B*—*X* system was first identified in the emission from the $Br_2 + ClO_2$ reaction.[43] Like IBr(*B*), and ICl(*B*), the *B* state of BrCl correlates with the lower energy spin–orbit product, and the higher energy vibrational levels are strongly perturbed by the interaction with the $Y(0^+)$ state (to the extent that no levels with $v' > 8$ have been seen in absorption or emission). Potential energy curves and Franck–Condon factors for the *B*—*X* system were derived from the spectroscopic data by Coxon.[44] The reason for the anomalous weakness of the absorption is clear from this work. The Franck–Condon factors for transitions from the thermally populated ground-state levels to the stable levels of the *B* state are very small (*e.g.*, $q_{v',v''} = 4.2 \times 10^{-5}$ for the 8—0 band).

In addition to the difficulties posed by the poor absorption of the bands, laser excitation studies of BrCl(*B*—*X* are complicated by the occurrence of four different isotopes ($^{79}Br^{35}Cl$, $^{81}Br^{35}Cl$, $^{79}Br^{37}Cl$, and $^{81}Br^{37}Cl$ with natural abundance ratios of 3:3:1:1), and the presence of equilibrium concentrations of Br_2. Clyne and McDermid[45] minimized the Br_2 concentration by mixing BrCl with a large excess of Cl_2 (typically 7:1, $[Cl_2]$:[BrCl]), enabling the observation of clean excitation spectra for the *B*—*X* system. Bands from $v'' = 1$ and 2 to $3 \leqslant v' \leqslant 7$ were recorded with full rotational resolution at a total pressure of about 5 torr. Fluorescence from

[42] M. A. A. Clyne, J. A. Coxon, and A. R. Woon-Fat, *Faraday Discuss. Chem. Soc.*, 1972, **53**, 82.
[43] M. A. A. Clyne and J. A. Coxon, *Proc. R. Soc. London, Ser. A*, 1967, **298**, 428.
[44] J. A. Coxon, *J. Mol. Spectrosc.*, 1974, **50**, 142.
[45] M. A. A. Clyne and I. S. McDermid, *J. Chem. Soc., Faraday Trans. 2*, 1978, **74**, 798.

transitions to $v' = 8$ could not be detected, and the fluorescence from $v' = 7$ was very weak. In fact, excitation of the $v' = 7$ bands could only be seen at relatively high pressures, where vibrational relaxation competes with the non-radiative decay, transferring a significant fraction of the excited-state population to stable levels. Spectra taken at pressures around 5 mtorr showed no evidence of $v' = 7$ bands,[46] and the onset of predissociation (indicated by the loss of rotational lines) was noted in the $v' = 6$ manifold at $J' = 42$ ($^{81}Br^{35}Cl$). A search was made for the onset in the $v' = 5$ manifold, but all of the observable levels ($J' < 70$) appeared to be stable.

Collision-free lifetime measurements[46] confirmed the sharp onset of predissociation at $v' = 6$, $J' = 42$. This result, coupled with the lower limit for the onset in $v' = 5$, was used to determine the type of curve crossing responsible for the predissociation. The $v' = 5$, $J' = 70$ level lies 149 cm^{-1} above $v' = 6$, $J' = 41$. Therefore the rotational barrier to predissociation is quite large, and this sets an upper limit of $r < 3.87$ Å for the internuclear distance of the curve crossing. From this limit Clyne and McDermid[46] argued that the predissociation was caused by a Herzberg case I(c) crossing (*cf.* Figure 5) involving a state of 0^+ symmetry. Their analysis provided an improved upper bound for the ground-state dissociation energy of $D_0^0(^{81}Br^{35}Cl) \leqslant 17\,960$ cm^{-1}.

Systematic measurements of the B state lifetime as a function of v', J', and pressure were carried out.[46,47] In the course of studying the pressure dependence it was found that the fluorescence-decay kinetics were strongly influenced by the effects of vibrational energy transfer. Consequently, the Stern–Volmer behaviour was studied under two sets of limiting conditions. At the high pressure limit ($P > 3$ torr) the fluorescence-decay curves were composed of a very fast, non-exponential decay at short times, followed by a fairly long-lived single exponential decay. The curves were interpreted in terms of an initial period of rapid vibrational relaxation, which eventually yields an equilibrium Boltzmann distribution among the vibrational levels. The long-lived component of the decay corresponds to the emission from the relaxed distribution. In accordance with this picture, the Stern–Volmer plots constructed from the tail of the decay were essentially independent of the vibrational level excited.[47] The rate constant for deactivation of BrCl(B) by the Cl_2/BrCl mixture was $(3.9 \pm 1.2) \times 10^{-13}$ cm^3 $molecule^{-1}$ s^{-1}, which is equivalent to a collision efficiency of about 2×10^{-3}. Fluorescence decay curves recorded in the low pressure limit (0.1—1.0 mtorr) were reasonably close to being single exponentials. The decay rates gave well defined, linear Stern–Volmer plots which were extrapolated to determine the collision-free lifetimes. For the stable levels ($1 \leqslant v' \leqslant 6$) a constant value of 40.2 ± 1.8 μs was found, regardless of the level excited. However, the deactivation rate constants were much larger than those observed in the high pressure experiments, and they showed a marked dependence on the vibrational energy. The rate constants increased smoothly from $(3.0 \pm 0.2) \times 10^{-12}$ cm^3 $molecule^{-1}$ s^{-1} for $v' = 1$,[48] up to $(2.1 \pm 0.4) \times 10^{-10}$ cm^3

[46] M. A. A. Clyne and I. S. McDermid, *Faraday Discuss. Chem. Soc.*, 1979, **67**, 316.
[47] M. A. A. Clyne and I. S. McDermid, *J. Chem. Soc., Faraday Trans. 2*, 1978, **74**, 807.
[48] M. A. A. Clyne and Lu Cheng Zai, *J. Chem. Soc., Faraday Trans. 2*, 1982, **78**, 1221.

molecule^{-1} s^{-1} for $v' = 6$.[46] Given the insensitivity of the lifetime to the quantum state and the small rate constant for electonic quenching, the origin of variation in the rate constant must be ascribed to vibrational energy transfer. This can either modify the fluorescence quantum yield by upward transfer to unstable levels, or decrease the detection sensitivity by downward transfer to levels which emit in the far-red spectral region. By use of a suitable photomultiplier/coloured glass filter combination, Clyne and McDermid[47] biased their detector to minimize the effect of downward energy-transfer on the detection sensitivity. In this way the deactivation caused by upward energy-transfer could be seen in isolation. Working under approximately single collision conditions[47] they noted extremely large rate constants for multiquantum vibrational energy-transfer events. For example, transfer from $v' = 3$ to $v' = 7$, a step which requires excitation energies in excess of 3.3 kT, occurred with a rate constant of 1.0×10^{-11} cm^3 molecule^{-1} s^{-1}.

The possibility for the extraction of energy-transfer rate constants from undispersed fluorescence decay measurements for BrCl(B) is a unique consequence of the delicate balance between the radiative decay rate and the energy-transfer rate, coupled with the existence of a sharp onset for predissociation and a low electronic quenching efficiency. This interesting combination of properties was also found in the B states of the remaining molecules to be discussed (BrF and Cl_2). The complex decay characteristics seen for BrCl(B), BrF(B), and $Cl_2(B)$ have been simulated by numerical integration of the appropriate rate equations. The results obtained by these methods are subject to a number of uncertainties as they are very model-dependent. The primary function of the model calculations has been to demonstrate the feasibility of the proposed mechanisms in a semi-quantitative fashion. This point should be borne in mind in considering the results presented in sections E, F, and G.

F. Bromine Monofluoride.—Prior to the laser excitation studies of Clyne, Curran, and Coxon,[49] the rotational structure of the BrF B—X system had not been resolved. Earlier investigators[50–52] observed vibrationally resolved spectra for this system in both emission and absorption. From the earlier work it was known that the B state correlates with the $Br\,^2P_{\frac{1}{2}} + F\,^2P_{\frac{3}{2}}$ atomic products [*cf.* IF(B)], and that the avoided crossing with the $Y(0^+)$ state causes predissociation of all levels above $v' = 8$. The laser excitation spectra[49] showed strong progressions from $v'' = 0$ to $3 \leqslant v' \leqslant 8$. The simple P and R branch structure confirmed the assignment of the electronic transition. A preliminary set of rotational constants were derived from these spectra, and the separations between the ^{79}BrF and ^{81}BrF band origins were used to confirm the the vibrational numbering. These parameters were later refined by Coxon and Curran,[53] who reinvestigated the absorption spectrum at a higher resolution.

The fluorescence decay dynamics of BrF(B) were first examined by Clyne and

[49] M. A. A. Clyne, A. H. Curran, and J. A. Coxon, *J. Mol. Spectrosc.*, 1976, **63**, 43.
[50] R. A. Durie, *Proc. R. Soc. London, Ser. A*, 1951, **207**, 388.
[51] P. H. Brodersen and J. E. Siece, *Z. Phys.*, 1955, **141**, 515.
[52] M. A. A. Clyne, J. A. Coxon, and L. W. Townsend, *J. Chem. Soc., Faraday Trans. 2*, 1972, **68**, 2134.
[53] J. A. Coxon and A. H. Curran, *J. Mol. Spectrosc.*, 1979, **75**, 270.

McDermid.[26,54,55] Ground-state BrF molecules were generated in a He carrier flow using the discharge flow system described previously. These studies were conducted at reasonably high pressures, requiring long extrapolations of the Stern–Volmer plots in order to determine the collision-free lifetimes. The deactivation rate constant for the gas mixture (predominantly He) was 3.8×10^{-12} cm^3 molecule^{-1} s^{-1}. From the lifetime measurements the onset of predissociation was located in the $v' = 7$ manifold near $J' = 30$. However, although relative magnitudes of the lifetimes were sufficiently well defined for the detection of predissociation, the absolute values were not reliable (lifetimes for $v' \leqslant 6$ were typically around 22 μs, whereas the actual collision-free lifetime is close to 60 μs). At total pressures in excess of 60 mtorr, the rotational energy transfer between stable and unstable rotational levels of the $v' = 7$ manifold produced markedly non-exponential decay curves, and the interpretation of these data constituted the most important aspect of the high pressure experiments.[54] Examples of the decay curves for $v' = 7$, $J' = 31$ are shown in Figure 16. All levels lying energetically close to the predissociation limit ($J' = 15$) exhibited decay curves with the same general characteristics as those in Figure 16. These curves could be approximately decomposed into a sum of two exponentials; an initial fast decay followed by a long-lived tail. As the energy of the level excited approached the predissociation limit, the fast decay gained intensity at

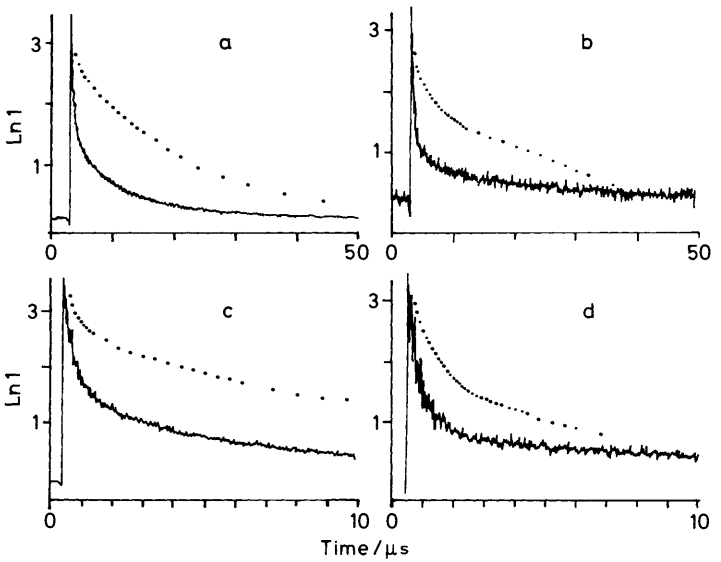

Figure 16 *Fluorescence decay curves for initial excitation of the $v' = 7$, $J' = 31$ level of ^{79}BrF(B). The points show the data plotted on a semi-log scale. Non-exponential decays are seen at both high and low pressure on 10 or 50 μs time-bases. (a) and (c) 326.2, (b) and (d) 141.8 mtorr* (Reproduced by permission from *J. Chem. Soc., Faraday Trans. 2*, 1978, **74**, 644)

[54] M. A. A. Clyne and I. S. McDermid, *J. Chem. Soc., Faraday Trans. 2*, 1978, **74**, 644.
[55] M. A. A. Clyne and I. S. McDermid, *J. Chem. Soc., Faraday Trans. 2*, 1978, **74**, 664.

the expense of the tail. This trend continued for the levels above the predissociation limit.

A simple computer model was used to simulate the $v' = 7$ decay curves.[54] Energy transfer between the various rotational levels was modelled using classical approximations. The model included the radiative decay rate determined for the $v' = 7, J' < 15$ levels and the deactivation rate constant from the measurements on the $v' < 6$ levels. The predissociation rate and the energy-transfer rate constant were treated as variable parameters. Simulations for excitation of levels below the predissociation limit indicated that the fast initial decay was caused by rotational 'ladder climbing' to the unstable levels. The apparent decay rate falls with time because the rotational population distribution moves towards an equilibrium state. Eventually a thermalized distribution is achieved which gives rise to the exponential 'tail' of the decay. When the initially excited level is predissociated, the model shows that the decay rate starts at a value which is close to the collision-free limit, but downward energy-transfer leads to population of the stable part of the manifold, and the decay rate decreases. Once again a constant decay rate was achieved when the population distribution reached equilibrium. The model calculations gave quantitative fits to the experimental decay curves when an energy-transfer rate constant of about 2.5×10^{-11} cm^3 molecule^{-1} s^{-1} was used.

Clyne and McDermid [54] found that the high pressure curves for the $v' = 8$ levels resembled those for $v' = 7$, but in this instance the cause of the non-exponential decay could not be attributed to rotational energy transfer. All of the $v' = 8$ levels were predissociated, with lifetimes that ranged from 1.63 μs for $J' = 4$ down to 0.11 μs for $J' = 31$. Stable levels could only be reached by vibrational relaxation, and numerical modelling of the kinetics provided a total vibrational-transfer rate constant of 2.5×10^{-11} cm^3 molecule^{-1}

Direct measurements of the collision-free lifetimes were made in the apparatus shown in Figure 6. In the first series of experiments [56] the fluorescence collimating lens was positioned at a distance of 17 mm from the laser axis. Lifetimes between 42–56 μs were seen for the $v' < 7$ levels, with a sharp drop to less than 100 ns at $v' = 6, J' = 49$, and $v' = 7, J' = 31$. As the onset of predissociation was observed in two vibrational manifolds the position of the maximum of the rotational barrier to dissociation could be estimated. The maximum was found to be at 5.34 ± 0.5 Å, which ruled out the possibility of a Herzberg type I(c) crossing (where the maximum would be somewhere near 2.5—3.0 Å), Thus the predissociation must proceed *via* the repulsive limb of a shallow bound state, in much the same way as it does for IF(*B*). As the curve crossing was of Herzberg's type I(b), the ground-state dissociation energy was established within close limits [$D_0^0(^{79}\text{BrF}) = 20\,622 \pm 20$ cm^{-1}].

The collision-free dynamics of the $v' = 8$ level were interesting as they were dissimilar to those of all the other levels. The entire manifold is considerably more stable than would be expected, given that all of its rotational states lie above the predissociation limit. For both isotopic species of BrF the decay rate was found to

[56] M. A. A. Clyne and I. S. McDermid, *J. Chem. Soc., Faraday Trans. 2*, 1978, **74**, 1376.

vary linearly with rotational energy for $J' = 4$ to 21. This behaviour is similar to that noted for the IF(B) $v' = 10$ level, and may be rationalized using similar arguments. Indeed, the collision-free dynamics of BrF(B) and IF(B) are closely related, and this is clearly a consequence of the correlation of the B states with the higher energy spin–orbit atomic products (*i.e.*, the more massive atom is spin–orbit excited).

A second series of experiments were conducted in the low pressure chamber in order to address the question of diffusional distortion of the decay curves. Clyne and Liddy[57] carefully examined the decay curves recorded with the apparatus shown in Figure 6, and they noted that the decay rate increased with time. Assuming that this was caused by diffusion, they modified the equipment by removing the fluorescence collection lenses and moving the detector to a position 37 mm away from the laser axis. With this configuration the low pressure decay curves were good single exponentials for the first 100 μs (diffusional distortion was apparent beyond 150 μs). Reliable lifetimes were obtained by analysing the data recorded on a 100 μs timebase. The lifetimes ($64.2 \geqslant \tau_r \geqslant 55.5$ μs for $7 > v' > 3$), were about 10 μs longer than those of the first low pressure study and there was a slight trend for the lifetime to decrease with decreasing v'. However, the transition dipole moment, calculated from equation 2, was independent of v' ($|R_e|^2 = 0.028$ D_2).

The high pressure experiments[55] had shown that the electronic quenching and ro-vibrational energy-transfer processes were convoluted when the decay dynamics were monitored by observing undispersed fluorescence. Ideally a deconvolution can be achieved by viewing the fluorescence from individual ro-vibrational levels through a monochromator, but the low intensity of the BrF(B) fluorescence makes this approach impractical. Clyne and Liddy[57] achieved a partial deconvolution by using band-pass and cut-off filters to monitor the fluorescence from small groups of levels. The final deconvolution was then accomplished by computer modelling of the resulting decay curves. This method is best described by considering the results for the deactivation of BrF(B) by O_2. Figure 17 shows a plot of the log of the fluorescence intensity (ln I) *vs.* time, following the excitation of the $v' = 6, J' = 21$ level of BrF(B) in the presence of 87 mtorr of O_2. At any point in this plot the gradient is proportional to the instantaneous decay rate (*i.e.*, $\mathrm{d}\ln I/\mathrm{d}t = -\Gamma$). The non-linear characteristics of Figure 17 can be explained in terms of vibrational energy transfer when the dependence of the detection sensitivity on v' is known. The sensitivity factors corresponding to the conditions used to record Figure 17 are shown in Figure 18. The initial fast decay of Figure 17 was caused by upward energy-transfer to unstable levels, and downward transfer to $v' = 5$, which is less sensitively detected than $v' = 6$ (*cf.* Figure 18). At longer times, vibrational relaxation populates levels in the range of $1 \leqslant v' \leqslant 4$. These are more efficiently detected than $v' = 6$, and so the decay rate slows down. This occurs in the region from 25 to 60 μs in Figure 17. Finally the decay rate increases slightly, reaching a constant value for the remainder of the observation period. As noted before, this final rate corresponds to emission from an equilibrium population distribution.

[57] M. A. A. Clyne and J. P. Liddy, *J. Chem. Soc., Faraday Trans. 2*, 1980, **76**, 1569.

Therefore, these data could be used to determine the rate constant for electronic quenching by O_2 ($k = 2.6 \times 10^{-12}$ cm^3 molecule^{-1} s^{-1}). The initial decay rates of the data recorded with the long-pass filter could be used to determine a lower limit for the rate constant for transfer out of $v' = 6$. A much more accurate value for this rate constant was obtained by using a band-pass filter to detect fluorescence from $v' = 6$ exclusively, but the experiments were difficult owing to the low signal levels transmitted by the filter. Clyne and Liddy[57] conducted a limited number of experiments using the band-pass filter, and for $v' = 6$ they found a total deactivation rate constant of 1.25×10^{-10} cm^3 molecule^{-1} s^{-1}. Estimates for the

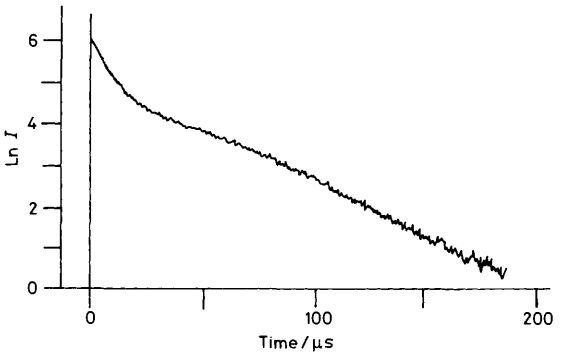

Figure 17 *Fluorescence decay of* BrF(*B*) *with* O_2 *as bath gas. Initial excitation was to the* $v' = 6$, $J' = 21$ *level of* ^{79}BrF(*B*). *Pressure of* O_2 = 87.0 mtorr. *Note the strongly curved, sigmoid-shaped logarithmic decay curve of undispersed fluorescence*
(Reproduced by permission from *J. Chem. Soc., Faraday Trans. 2*, 1980, **76**, 1569)

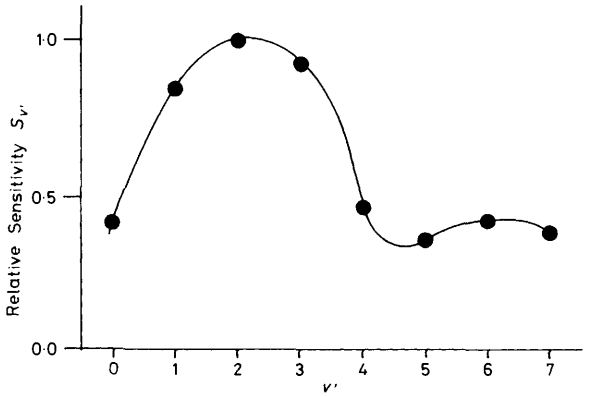

Figure 18 *Variation of detector sensitivity with vibrational state in* BrF(*B*). *The detector consisted of a Kodak-Wratten 23A filter and EMI 9558 photomultiplier*
(Reproduced by permission from *J. Chem. Soc., Faraday Trans. 2*, 1980, **76**, 1569)

individual state-to-state rate constants [$k(v' \longrightarrow v' \pm 1)$] were then deduced from the directly determined rate constants and the convoluted decay curves by computer modelling. The results indicated that the vibrational energy-transfer rates decreased with decreasing v', in general agreement with Troe's[58] model for vibrational energy transfer.

Clyne and Liddy[57] also investigated the deactivation of BrF(B) by a number of other collision partners (Ar, Cl_2, HCl, and $CHFCl_2$). With the exception of HCl, these collision partners produced non-exponential decay curves, but the characteristics of these curves were quite different from those seen in Figure 17. Using computer modelling it was demonstrated that all of these data could be accounted for by the vibrational energy transfer. The reader is referred to reference 57 for further details of this work.

G. Chlorine.—The extensive photochemistry of chlorine atoms, initiated through optical dissociation or predissociation of Cl_2 at wavelengths below 500 nm, has been the motivation for many studies of the Cl_2 B—X and continuum absorption systems. Much of this work has been reviewed by Coxon,[1] and the data for the B—X system have been further discussed by Clyne and McDermid.[4]

The B—X system is easily resolved and particularly simple in its appearance, despite the presence of three isotopic species [$^{35}Cl^{35}Cl$ (57%), $^{35}Cl^{37}Cl$ (37%), $^{37}Cl^{37}Cl$ (6%)]. In absorption the most intense region of the $v'' = 0$ progression terminates on the $14 \leqslant v' \leqslant 24$ levels of the B state. However, Clyne and McDermid[59] were unable to record laser excitation spectra for these levels (at a Cl_2 pressure of 20 mtorr) and spectra could only be seen when excitation wavelengths greater than 501 nm were used. Between 501 and 504 nm a number of bands terminating on $5 \leqslant v' \leqslant 12$ were observed. The intensity of the spectrum fell rapidly with increasing wavelength, in keeping with the very small Franck–Condon factors for excitation to the lower vibrational levels. At the short wavelength limit of the spectrum the onset of predissociation at $v' = 12, J' = 21$ ($^{35}Cl_2$) was apparent, and both the 12—0 and 11—0 bands were less intense than expected. The fluorescence quantum yields for these levels were reduced by collisional destabilization (see below).

Instrumental problems were encountered in the first attempts to measure the relatively long lifetime of the B state. Clyne and McDermid[60] recorded fluorescence decay curves for several of the stable levels ($v' \leqslant 12$) using Cl_2 pressures of 0.22—1.01 mtorr. Even at the lowest pressures, collision-free measurements could not be achieved. The Stern–Volmer plots gave an average radiative lifetime of 85 μs, although the deactivation rate constants were strongly dependent on v'. In the apparatus used for these studies the detector window was positioned 17 mm away from the laser axis. The average thermal velocity of Cl_2 at room temperature is 3.3×10^4 cm s^{-1}, so the average time for the excited molecules to reach the detector window was about 50 μs. On this basis a distortion of the

[58] J. Troe, *J. Chem. Phys.*, 1977, **66**, 4745.
[59] M. A. A. Clyne and I. S. McDermid, *J. Chem. Soc., Faraday Trans. 2*, 1978, **74**, 1935.
[60] M. A. A. Clyne and I. S. McDermid, *J. Chem. Soc., Faraday Trans. 2*, 1979, **75**, 280.

fluorescence decay curves, consisting of a steady increase in the decay rate after 50 μs, would be expected. Unfortunately this was masked by the high noise level which accompanied the very weak fluorescence signals. The effects of diffusion were more clearly evident in the experiments performed by Clyne and Martinez.[61] In this work the signal strength was increased by the use of a more powerful excitation laser, and a large diameter vacuum chamber was employed. The detector could be placed in one of two positions in this apparatus; a normal position, with a distance of 125 mm between the detector and the laser axis, and a forward position where this distance was reduced to 25 mm. The longest lifetime recorded with the detector in the forward position was 160 μs. At pressures below 2 mtorr the mean free path exceeds 25 mm, and the lifetime actually decreases in going from 2 to 0.3 mtorr. Decay curves which were unaffected by diffusion were recorded with the detector in the normal position. The longest directly measured lifetime was 260 μs, and a short Stern–Volmer extrapolation gave a collision-free lifetime of 305 ± 15 μs. This corresponds to a transition dipole moment of $|R_e|^2 = 0.011\ D^2$.

Excitation spectra for the levels with $v' > 12$ could not be seen at low Cl_2 pressures, but Clyne and McDermid[62] found that they could detect some of the low J' lines of the $v'' = 0 \longrightarrow 13 \leqslant v' \leqslant 25$ bands when the pressure was increased to 40 mtorr. The intensity contours of these bands indicated a strong rotationally dependent predissociation. Lifetime measurements for $v' \geqslant 13$ were made at a fixed Cl_2 pressure of 50 mtorr. Within each vibrational manifold the decay rates varied linearly with rotational energy, and the fits to the heterogeneous predissociation rate expression (equation 5) were excellent. The predissociation rate constants, k_v, were much larger than those seen for $Br_2(B)$ (by a factor of ~ 100) and did not show the same oscillating dependence on the vibrational level (*cf.* Figures 14 and 19). Rotation-free lifetimes were measured by excitation of the $P(1)$ lines (where $J' = 0$), which were easily identified in the excitation spectrum. Clyne and McDermid[62] obtained values around 670 ns for all of the vibrational levels studied, and the agreement between the measurements and the intercepts extrapolated from equation 5 was generally good. This implied the presence of a strong homogeneous interaction, which is very difficult to account for. Of the 21 Hund's case (c) states that correlate with the $^2P_J + {}^2P_J$ atomic products the B state is the only 0_u^+ state. Hence all of the energetically feasible homogeneous interactions are symmetry forbidden. Clyne and McDermid[62] suspected that their results could have been influenced by upward rotational energy-transfer, but this could not be checked as the available laser power did not permit the use of very low pressures. This ambiguity was resolved in studies conducted in the more sensitive equipment used by Clyne and Martinez.[63] For the $v' = 13$, $J' = 0$ level, a lifetime of 14.3 μs was seen at 4.8 mtorr, and a Stern–Volmer extrapolation to zero pressure showed that this level was unaffected by predissociation in accordance with the theoretical expectations. Although the new low pressure measurements revised the positions of the intercepts for the plots of decay rate *vs.* rotational energy, they yielded

[61] M. A. A. Clyne and E. Martinez, *J. Chem. Soc., Faraday Trans. 2*, 1980, **76**, 1275.
[62] M. A. A. Clyne and I. S. McDermid, *J. Chem. Soc., Faraday Trans. 2*, 1979, **75**, 1677.
[63] M. A. A. Clyne and E. Martinez, *J. Chem. Soc., Faraday Trans. 2*, 1980, **76**, 1561.

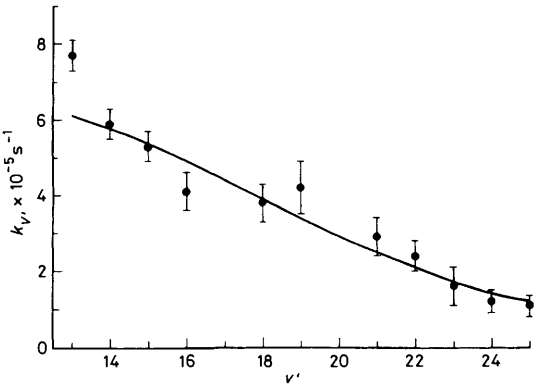

Figure 19 $Cl_2(B)$ *predissociation rate constants as a function of the vibrational level v'. Solid circles (●) are the experimental data points, with error bars which correspond to one standard deviation. Calculated* $k_{v'}$ *values are represented by the smooth curve*
(Reproduced by permission from *J. Chem. Soc., Faraday Trans. 2*, 1982, **78**, 1339)

predissociation rate constants which were close to those determined in the earlier study.[62]

The theoretical implications of the $Cl_2(B)$ predissociation behaviour were further investigated by Heaven and Clyne.[64] Symmetry considerations limit the possible assignments for the state responsible for the predissociation to $A^3\,\Pi\,(1_u)$ or $^1\Pi\,(1_u)$. The predissociations in both $I_2(B)$ and $Br_2(B)$ are mediated by the latter, and it would seem reasonable to assume that this is also the case for $Cl_2(B)$. However, the details of the quantum state dependence of the predissociation rate do not support this assignment. The $^1\Pi\,(1_u)$ state correlates with ground-state atomic products, and it must cross the attractive limb of the *B* state [as it does for $Br_2(B)$, *cf.* Figure 3]. The onset of predissociation for this Herzberg's type I(c) crossing would lie at an energy above that of the ground-state dissociation limit, while the $k_{v'}$ values would show large variations for the first few levels above the crossing point. In contrast, the first level of $Cl_2(B)$ above the ground-state dissociation limit is unstable and, as Figure 19 shows, the $k_{v'}$ values decreased smoothly with increasing v'. These characteristics can only be produced by predissociation *via* a bound state, making the assignment of this state to $A^3\,\Pi\,(1_u)$ unambiguous. Heaven and Clyne[64] estimated the form of the *A* state potential energy curve by calculating the pattern of $k_{v'}$ values (using equation 6) and adjusting the potential until the experimental pattern was approximated. The results were consistent with the limited spectroscopic data available for the *A* state.

Ro-vibrational energy-transfer processes dominate the collisional deactivation kinetics of $Cl_2(B)$. Clyne and McDermid[65] found that the self-deactivation rate

[64] M. C. Heaven and M. A. A. Clyne, *J. Chem. Soc., Faraday Trans. 2*, 1982, **78**, 1339.
[65] M. A. A. Clyne and I. S. McDermid, *J. Chem. Soc., Faraday Trans. 2*, 1979, **75**, 1313.

constant, measured under single collision conditions, decreased with increasing energy separation from the predissociation limit [$k(v' = 12) = 3.9$, $k(11) = 2.4$, $k(10) = 1.2$, $k(9) = 0.6 \times 10^{-10}$ cm^3 molecule^{-1} s^{-1}]. As for BrCl(B), the primary deactivation mechanism was upward vibrational energy-transfer to unstable levels. In order to decompose the deactivation rate constants into approximate state-to-state rate constants, a simple model was proposed. It was assumed that the state-to-state transfer probabilities were controlled by the change in the vibrational quantum number (Δv), and that they were insensitive to the initial vibrational state. Thus each deactivation rate could be expressed as a sum of the rates for upward transfer to the unstable levels *i.e.*,

$$\begin{aligned} k(12) &= k(\Delta v = 1) + k(\Delta v = 2) + k(\Delta v = 3) + \ldots . \\ k(11) &= \qquad\quad k(\Delta v = 2) + k(\Delta v = 3) + \ldots . \end{aligned}$$

Differences between the measured rate constants then define the state-to-state rate constants [$k(\Delta v = 1) = 1.5$, $k(\Delta v = 2) = 1.2$, $k(\Delta v = 3) = 0.5 \times 10^{-10}$ cm^3 molecule^{-1} s^{-1}]. Once again the probabilities for multi-quantum upward energy-transfer are surprisingly large.

Rate constants for direct electronic quenching of $Cl_2(B)$ $v' < 12$ were found to be small for all of the collision partners investigated [$Cl_2(X)$, N_2, O_2, and Ar].[61] The electronic quenching was measured by using a high bath-gas pressure, and analysing the segment of the fluorescence decay which corresponded to emission from a thermalized population distribution (even with excitation to levels as low in energy as $v' = 5$ these measurements needed correction for the contribution from energy transfer). For self deactivation, a quenching rate constant of 6.4×10^{-12} cm^3 molecule^{-1} s^{-1} was found, while the rate constants for N_2 and O_2 were less than 1.0×10^{-11} cm^3 molecule^{-1} s^{-1}. Quenching by Ar was immeasurably slow.

The inefficient electronic quenching of the stable levels of $Cl_2(B)$ is consistent with the trends for the other halogens and interhalogens. Rapid electronic self-quenching is only seen for $Br_2(B)$ and $I_2(B)$, where deactivation can proceed by collision-induced predissociation. This channel must be open for the $v' > 12$ levels of $Cl_2(B)$, but its contribution to the total deactivation rate constant is difficult to assess. Clyne and Martinez[63] found a deactivation rate constant of 2.8×10^{-10} cm^3 molecule^{-1} s^{-1} following excitation to $v' = 13$, $J' = 0$, and this defines an upper limit for self quenching. However, it is known that rotational energy transfer also deactivates this state, but the relative importance of this channel has not been determined.

7 Summary

The radiative lifetimes of the diatomic halogen and interhalogen $B^3\pi(0^+)$ states range from about 1μs for I_2 to 350μs for ClF. The lifetimes show a systematic dependence on the extent of spin–orbit coupling and mixing of the low-lying electronic states. This leads to an approximate correlation between the reciprocal lifetime and the molecular mass. Mixing of the valence states results in predissociation of the higher energy levels of all of the halogen and interhalogen B states. Because of the u/g symmetry restriction the halogens are exclusively

predissociated by 1_u states. $I_2(B)$ and $Br_2(B)$ are predissociated by the purely repulsive $^1\pi(1_u)$ states, while $Cl_2(B)$ suffers predissociation *via* the repulsive limb of the $A^3\Pi(1_u)$ state. The pronounced vibrational dependence of these heterogeneous decay channels has been used to characterize quantitatively the repulsive potential energy curves. A strong interaction with a repulsive $Y0^+$ state causes extensive perturbation of the interhalogen B states. In all cases this results in a very rapid predissociation of the B state at energies above the curve crossing. At energies between the crossing point and the ground state dissociation limit a weaker predissociation is observed. This channel exhibits both homogeneous and heterogeneous characteristics. A summary of the collision-free fluorescence decay rate data for the halogen and interhalogen B states is given in Table 2.

Self-quenching rates and the rates of quenching by common molecular gases are generally found to have a low collisional efficiency, although collisional predissociation, as studied in $Br_2(B)$ and $I_2(B)$, has a collisional efficiency approaching unity. The subtle effects of vibrational and rotational energy transfer on the fluorescence decay dynamics have been exploited to provide estimates for the energy-transfer rate constants. Vibrational and rotational energy transfer within the B states appear to be very efficient processes, occurring with near gas-kinetic rate constants for a wide variety of collision partners.

8 Recent Progress

The work summarized in this review, taken with the results from contemporary studies, has laid the foundations for an understanding of the dynamics of the halogen and interhalogen B states. A great deal has been learned about the delicate balance between radiative, predissociative, and collisional processes in this family of closely related electronic states. As always, many important questions remain unanswered, and much of the current research is directed towards a more detailed probing of the collision dynamics. To conclude, I would like to indicate briefly the way in which the results from Michael Clyne's laboratory have been used and extended in recent years.

The IF B—X transition has received the most attention, as it was clear from the lifetimes and deactivation rate constants that this system could be used to produce a chemically pumped laser. Davis *et al.*[66–68] have demonstrated both pulsed and continuous wave lasing of IF by optically pumping the B—X transition. At pressures above 1 torr they noted lasing from collisionally populated levels, and this observation initiated further studies of the collision dynamics for IF(B). Wolf and co-workers[69,70] have measured rate constants for quenching of IF(B) by He, Ne, Ar, Kr, Xe, N_2, F_2, I_2, O_2, H_2O, and SF_6. Vibrational energy-transfer rate constants were also measured[69] for collisions of IF(B) with He and N_2. Chemiluminescent reactions which produce IF(B) have been analysed using the

[66] S. J. Davis and L. Hanko, *Appl. Phys. Lett.*, 1980, **37** 692.
[67] S. J. Davis, L. Hanko, and R. F. Shea, *J. Chem. Phys.*, 1983, **78**, 172.
[68] S. J. Davis, L. Hanko, and P. J. Wolf, *J. Chem. Phys.*, 1985, **82**, 4381.
[69] P. J. Wolf, J. H. Glover, L. Hanko, R. F. Shea, and S. J. Davis, *J. Chem. Phys.*, 1985, **82**, 2321.
[70] P. J. Wolf and S. J. Davis, *J. Chem. Phys.*, 1985, **83**, 91.

results of Clyne and McDermid.[22,26,32] The reactions investigated include (reference numbers given in square brackets):

$F_2 + I_2 + O_2\ (^1\Delta_g)$	[71]
$F + I_2 + HN_3$	[72]
$IF(X) + N_2\ (A\ ^3\Sigma_u^+)$	[73]

Reactions which produce $IF(X)$ can be conveniently followed by LIF, and at sufficiently low pressures information about the vibrational energy content of the newly formed IF may be obtained. LIF probing has been used to study the reactions:

$F_2 + I_2$	[74]
$F + I_2$	[75, 76]
$F + ICl$	[76]
$F + IBr$	[76]
$O + CF_3I$	[77]

Predissociation of $Br_2(B)$ by hyperfine interactions has been characterized by Koffend *et al.*[78] and Siese *et al.*[79] Both groups resolved the hyperfine structure of the rotational lines by using molecular beam techniques to minimize the Doppler linewidth. The Br_2 B—X system has also been optically pumped to lasing, first by Wodarczyk and Schlossberg,[80] and more recently by Perram and Davis.[81] The latter investigators modelled the kinetics associated with optical pumping and found that the self-quenching and energy-transfer rate constants of Clyne *et al.*[40] were too large to be compatible with the pressure *vs.* output power curves for the laser. van de Burgt and Heaven[82] have subsequently measured the $Br_2(B)$ self-quenching rates for a wide range of pressures. Their quenching rate constants were in good agreement with those of Clyne *et al.*,[40] and high efficiencies for energy transfer were observed. Energy-transfer channels were not included in the optical pumping model, and this may be the source of the discrepancy between the calculations and the laser performance.[82]

Kenner and Ogryzlo[3] have used the predissociation rate data for $Cl_2(B)$ and $Br_2(B)$ to analyse the chemiluminescent reactions:

$$Cl + Cl + M \longrightarrow Cl_2(B) + M$$
$$Br + Br + M \longrightarrow Br_2(B,A) + M$$

[71] P. D. Whitefield, R. F. Shea, and S. J. Davis, *J. Chem. Phys.*, 1983, **78**, 6793.
[72] A. T. Pritt, Jr., D. Patel, and D. J. Benard, *Chem. Phys. Lett.*, 1983, **97**, 471.
[73] L. G. Piper, W. J. Marinelli, W. T. Rawlins, and B. D. Green, *J. Chem. Phys.*, 1985, **83**, 5602.
[74] P. D. Whitefield and S. J. Davis, *Chem. Phys. Lett.*, 1981, **83**, 44.
[75] R. J. Donovan, D. P. Fernie, M. A. D. Fluendy, R. M. Glen, A. G. A. Rae, and J. R. Wheeler, *Chem. Phys. Lett.*, 1980, **69**, 472.
[76] T. Trickl and J. Wanner, *J. Chem. Phys.*, 1983, **78**, 6091.
[77] T. A. Watson, M. Addison, and C. Wittig, *Chem. Phys.*, 1983, **78**, 57.
[78] J. B. Koffend, R. Bacis, S. Churassy, M. L. Gaillard, J. P. Pique, and F. Hartmann, *Laser Chem.*, 1983, **1**, 185.
[79] M. Siese, E. Tiemann, and U. Wulf, *Chem. Phys. Lett.*, 1985, **117**, 208.
[80] F. J. Wodarczyk and H. R. Schlossberg, *J. Chem. Phys.*, 1977, **67**. 4476.
[81] G. P. Perram and S. J. Davis, *J. Chem. Phys.*, 1986, **84**, 2526.
[82] L. J. van de Burgt and M. C. Heaven, *Chem. Phys.*, 1986, **103**, 407.

Assuming that these reactions occur by the inverse of spontaneous and collision-induced predissociation, they calculated the rate constants for bimolecular and termolecular recombination. The results for Cl indicate that these processes account for only a small fraction of the $Cl_2(B)$ produced. However, inverse predissociation does adequately account for the $Br_2(B)$ produced in the Br atom recombination.

Chlorine monofluoride was the only interhalogen not studied in Clyne's laboratory. Laser excitation spectra for ClF *B*—*F* were first recorded by McDermid[83] and McDermid and Laudenslager.[84] Interesting rotational perturbations of the *B* state were noted in the $v' = 7$, 8, and 9 manifolds, but no attempt was made to obtain kinetic data. The radiative lifetime of the *B* state has been measured by van de Burgt and Heaven.[85] From a short Stern–Volmer extrapolation they obtained a lifetime of 0.35 ± 0.15 ms and an effective self-deactivation rate constant of 2.3×10^{-11} cm^3 molecule^{-1} s^{-1}.

The well characterized laser excitation spectra of the halogens and interhalogens have been exploited in experiments where the molecules are used as fluorescent probes. This approach has been used to monitor the cooling processes in supersonic free-jet expansions, where rotationally resolved LIF spectra are used to determine local vibrational and rotational temperatures. To date, the free-jet cooling of I_2,[86,87] Br_2,[88] BrCl,[89] BrF,[90] IF,[90] and ICl[91] has been investigated for a variety of carrier gases. Some of the results (notably those for I_2, Br_2, and BrCl) are consistent with a large increase in the cross section for vibrational relaxation at very low temperatures. This trend is in contrast to the predictions of simple theoretical models, but it may be explained by the formation of long-lived collision complexes.

The extreme cooling in a free-jet expansion (temperatures below 1K are easily achieved) often leads to the formation of weakly bound van der Waals complexes.[92] The complexes formed between halogens and rare-gas atoms have been studied in some detail. The low-lying electronic states of the molecules are very weakly perturbed by the van der Waals interaction, and the complexes can be detected using the *B*—*X* transitions. Work on the complexes of I_2 has been reviewed by Levy.[93] Excitation spectra have also been recorded for $HeBr_2$,[94] $NeBr_2$,[95] $HeCl_2$,[96] $NeCl_2$,[97]

[83] I. S. McDermid, *J. Chem. Soc., Faraday Trans. 2*, 1981, **77**, 519.
[84] I. S. McDermid and J. B. Laudeaslager, *Chem. Phys. Lett.*, 1981, **79**, 370.
[85] L. J. van de Burgt and M. C. Heaven, to be published.
[86] G. M. McClelland, K. L. Saenger, J. J. Valentini, and D. R. Herschbach, *J. Chem. Phys.*, 1979, **83**, 947.
[87] M. Sulkes, J. Tusa, and S. A. Rice, *J. Chem. Phys.*, 1980, **72**, 5733.
[88] S. J. Bullman, J. W. Farthing, and J. C. Whitehead, *Mol. Phys.*, 1981, **44**, 97.
[89] J. W. Farthing, I. W. Fletcher, and J. C. Whitehead, *Mol. Phys.*, 1983, **48**, 1067.
[90] J. W. Farthing, I. W. Fletcher, and J. C. Whitehead, *J. Phys. Chem.*, 1983, **87**, 1663.
[91] S. G. Hansen, J. D. Thompson, R. A. Kennedy, and B. J. Howard, *J. Chem. Soc., Faraday 2*, 1982, **78**, 1293.
[92] See, for example, S. K. Grey and S. A. Rice, *J. Chem. Phys.*, 1985, **83**, 2818.
[93] D. H. Levy, in 'Photoselective Chemistry', ed. J. Jortner, R. D. Levine, and S. A. Rice, John Wiley, 1981, p. 323.
[94] L. J. van de Burgt, J. P. Nicolai, and M. C. Heaven, *J. Chem. Phys.*, 1984, **81**, 5514.
[95] B. A. Swartz, D. E. Brinza, C. M. Western, and K. C. Janda, *J. Phys. Chem.*, 1984, **88**, 6272.
[96] J. I. Cline, D. D. Evard, F. Thommen, and K. C. Janda, *J. Chem. Phys.*, 1986, **84**, 1165.
[97] D. D. Evard, F. Thommen, and K. C. Janda, *J. Chem. Phys.*, 1986, **84**, 3630.

and HeICl.[98] These simple complexes are prototype systems for investigating the nature of the van der Waals bond and for the study of photodissociation dynamics on a single adiabatic potential energy surface. The latter process has proved to be particularly amenable to theoretical treatment.

Acknowledgements. I am indebted to the late Dr. Michael A. A. Clyne for the training, encouragement, and support which he provided throughout the years of our association. It was a pleasure and privilege to work with him. I also wish to thank Dr. L. J. van de Burgt for his helpful criticism of this manuscript, and the Air Force Office of Scientific Research for their past and present support of the work described in this review.

[98] J. M. Skene and M. I. Lester, *Chem. Phys. Lett.*, 1985, **116**, 93.